A STUDY OF ENERGY LEVELS IN ODD-MASS YTTERBIUM ISOTOPES BY MEANS OF (d, p) AND (d, t) REACTIONS

BY

D. G. BURKE, B. ZEIDMAN, B. ELBEK,

B. HERSKIND, AND M. OLESEN

CONTENTS

Synopsis

The results of an experimental study of (d,p) and (d,t) reactions with 12 Mev deuterons on targets of Yb^{168}, Yb^{170}, Yb^{172}, Yb^{174} and Yb^{176} are reported. A magnetic spectrograph was used to analyze the reaction products with an overall energy resolution of $\sim 0.1\,^0/_0$. The observed populations of the low-lying states in the final odd nuclei are in general agreement with predictions based on the stripping theory for deformed nuclei, made by the use of the Nilsson wave functions and single-particle cross sections obtained from a distorted wave Born approximation calculation.

The relative populations of the various members of a rotational band based on an intrinsic state are highly characteristic of the state, and change only slightly from one nucleus to another. This property permits the unambiguous assignment of all the low-lying orbitals, except those with very weak cross sections, without the necessity of measuring angular distributions.

Many previously unknown levels have been found in the present work, and approximately fifty of them have been classified in terms of the Nilsson model. In addition, some speculations concerning vibrational states have been made. The use of the complementary reactions is shown to be a useful technique for determining the hole or particle character of the states. The filling of the orbitals as a function of mass number is in good agreement with pairing theory predictions, and indicates that the pairing energy parameter, $\varDelta$, is 0.80 ± 0.15 Mev.

1. Introduction

The amount of experimental information concerning the excited states of deformed odd nuclei has increased considerably in recent years together with an improvement of the theoretical description of these states. The low-lying states can be described remarkably well as collective rotations based on single-particle orbitals in a deformed potential[1, 2]. Some success has also been obtained in interpreting certain states at higher excitation as collective vibrations based on the single-particle levels. These collective states can be considered to be the result of a correlated motion of many particles where, in the limiting case, the amplitude of each single-particle component is small compared to the total. However, in actual fact, collective vibrational states often exhibit properties which indicate that one or two single-particle components may constitute appreciable fractions of the total amplitude. In order to understand the properties of these states, it would be useful to have a knowledge of the systematics of intrinsic states and the composition of the collective states in this region.

As a result of the various different modes of excitation the energy spectrum of a heavy deformed nucleus can be very complex. For the experimental study of such spectra, it is advantageous to make use of nuclear reactions with a high degree of selectivity in the nature of the states populated. Thus, it is well known that reactions involving the transfer of a single nucleon between projectile and target are especially suited for the determination of the various single-particle components of a state which, in principle, can be determined from the reaction cross sections.

In the past, (d, t) and (d, p) reactions have been used to study low-lying levels in several nuclei which have a spherical equilibrium shape[3, 4]. The two reactions serve as complementary spectroscopic tools in that the stripping process favours the population of particle states whereas the pick-up process favours the population of hole states. A number of deformed nuclei have also been studied by means of the (d, p) reaction[5, 6, 7] and it has been

1*

shown that the probabilities for populating the various members of rotational bands can be predicted quite well, using the stripping theory of SATCHLER[8] with the nuclear wave functions of NILSSON[1] and the intrinsic-particle cross section given by a distorted wave Born approximation (DWBA) calculation[9]. It is not a priori expected that such is the case, since all three basic parts of the analysis do not have a sound theoretical footing. In the form used, the Satchler stripping theory is valid only insofar as the reaction proceeds by a one step process. For the deformed nuclei, the presence of a large number of low-lying easily excited rotational levels provides a region where the two-step process of excitation and stripping may be important. It will be shown however, in an unambiguous case, that this mechanism is not of primary importance. The use of Nilsson wave functions based upon a harmonic oscillator potential is justified by the success achieved using these wave functions. More realistic wave functions would be obtained from calculations in a deformed Woods-Saxon well, but the qualitative features of the wave functions must be retained, i.e. large components of the wave function must remain large, small components remain small. DWBA calculations that have been used to date assume a zero-range interaction and spherical nuclei. It would be desirable to have coupled channel calculations that treat finite-range, non-locality and spin-orbit coupling in a deformed system while utilizing optical model parameters obtained from an extensive series of experiments and analysis. The complexity of this problem places it beyond the current range of detailed calculation. It has been shown, however, that the zero-range calculation provides good qualitative relationships among the cross sections for different l-values and Q-values, provided reasonable optical model parameters are used[5, 6]. If sufficient information is available, this feature makes it possible to extract detailed absolute information once the procedure has been calibrated. This has been done in the present study. Information was available prior to analysis for several low-lying intrinsic bands. This information was used in an empirical analysis of some of the data from both (d,p) and (d,t) reactions and the results were compared with those obtained with the procedures outlined above. Cross-checks and consistency between the two methods of analysis together with consistency in the results obtained from the analysis of all the data show that the procedures are reliable. We can therefore state that despite the theoretical objections that can be raised, the procedures used yield meaningful identifications and spectroscopic factors. In the discussion to follow, it is therefore tacitly assumed that use of the Satchler stripping theory, Nilsson wave functions and representative zero-range DWBA calcu-

lations is justified and may be utilized as a framework within which to analyze the data.

The present work is part of an investigation of the energy levels in the ytterbium nuclei by means of the (d,p) and (d,t) reactions. The analysis of the results for the even-even final nuclei will appear as a separate report[10]. In order to examine the systematic behaviour of the intrinsic states and their filling near the Fermi surface it is helpful to carry out experiments on a series of isotopes. Therefore, targets enriched in each of the stable isotopes of ytterbium were used. The ytterbium series, where there are seven stable isotopes (five even-even and two odd), was chosen because there is very little variation in nuclear deformation[11]. Also, the vibrational states in the heavier ytterbium nuclei are at higher excitation energies than in other rare earths[10, 12]. Thus, it is expected that they will have less interaction with the low-lying intrinsic states populated by the stripping and pick-up processes, making possible the observation of relatively pure single-particle states over a greater interval of excitation.

2. Theoretical Considerations

From the work of SATCHLER[8] it is seen that the differential cross section for a (d,p) reaction between a target nucleus with spin I_i and a final state with spin I_f can be written

$$\frac{d\sigma}{d\omega} = \frac{2I_f + 1}{2I_i + 1} \sum_l S_l \varphi_l(\theta),\tag{1}$$

where $\varphi_l(\theta)$ is the single-particle reaction cross section for angular momentum transfer l at the angle θ. This quantity can be obtained by means of a distorted wave Born approximation (DWBA) calculation.

The spectroscopic factor, S_l, is determined by the nuclear structure only, and is thus independent of angle θ, Q-value, etc. If one uses the Nilsson wave functions[1], the value of S_l for a transition to a rotational state in a deformed nucleus is

$$S_l = \sum_j \theta_{jl}^2,\tag{2}$$

where

$$\theta_{jl} = g \sqrt{\frac{2I_i + 1}{2I_f + 1}} \langle I_i j \pm K_i \mp \Delta K | I_f K_f \rangle C_{jl} \langle \varphi_i | \varphi_f \rangle.\tag{3}$$

The C_{jl} values are characteristic of the orbital into which the neutron is stripped and are related to the Nilsson coefficients $a_{l\Lambda}$ by means of the Clebsch-Gordon transformation

$$C_{jl} = \sum_{\Lambda} a_{l\Lambda} \langle l\tfrac{1}{2}\Lambda\Sigma | j\Omega \rangle, \tag{4}$$

where the quantities Λ, Σ, K and Ω are the same as those used by NILSSON. K_i and K_f are the spin components parallel to the symmetry axis in the initial and final nucleus, respectively. ΔK is the K value of the orbital into which the neutron is stripped. $\langle \varphi_i |_f \varphi \rangle$ is the overlap integral for the initial and final states and is expected to be nearly unity if the nuclear deformation does not vary greatly. The factor g is equal to $\sqrt{2}$ if $K_i = 0$ or $K_f = 0$ but otherwise is equal to unity.

In general, the reaction cross section to a given state can have contributions from several different l-values. However, for an even-even target nucleus where j is necessarily equal to I_f the expression simplifies to

$$\frac{d\sigma}{d\omega} = 2C_{jl}^2 \varphi_l. \tag{5}$$

In this case it is therefore much easier to compare the theoretical and experimental results, and it is for this reason that the experiments pertaining to levels in odd nuclei are discussed first. It is then possible to use empirical values of $C_{jl}^2 \varphi_l$ to make better predictions for the population of states in even-even nuclei.

The above discussion neglects the partial filling of levels caused by the pairing force and assumes that $U^2 = 1$, where U^2 is the probability that the state into which the neutron is stripped is empty in the target nucleus. Therefore, expression (5) should be changed to read

$$\frac{d\sigma}{d\omega} = 2C_{jl}^2 \varphi_l U^2. \tag{6}$$

All the expressions (1)–(6) are valid also for the (d,t) reaction, provided an appropriate φ_l is used and U^2 is changed to V^2, where $U^2 + V^2 = 1$. The C_{jl} coefficients in this case pertain to the state from which the neutron is removed.

3. Experimental Procedure and Results

The 12-Mev deuteron beam used in these experiments was produced by the Niels Bohr Institute Tandem Accelerator. The reaction products were analyzed in a single gap, broad range, magnetic spectrograph[13]. Targets of Yb, isotopically enriched in the desired mass number, were prepared by vacuum evaporation onto carbon backings from a tantalum crucible heated by electron bombardment[14]. The enriched samples were obtained in the form of Yb_2O_3 from the Stable Isotopes Division of the Oak Ridge National Laboratory and the isotopic compositions estimated by the supplier are shown in Table 1. Before evaporation, the oxides were reduced by lanthanum to ytterbium metal. The target thickness was between 50 $\mu g/cm^2$ and 150 $\mu g/cm^2$. The Yb^{168} target was not prepared in the above manner, because of the low natural abundance of this isotope (0.2 %). For this target, a sample enriched to $\sim 10\%$ Yb^{168}, obtained from Oak Ridge, was subjected to further enrichment in the University of Aarhus isotope separator, and simultaneously deposited on a carbon backing by the technique developed by SKILBREID[15]. The final enrichment is estimated to be ~ 99 % and the thickness was ~ 40 $\mu g/cm^2$.

The beam defining slits and the entrance aperture of the spectrograph were set to give an energy resolution of approximately 0.1 %. The solid angle of the spectrograph varies slightly with plate position and this dependence was determined by placing a ThB alpha source in the target position and, using different magnetic field strengths, making short exposures of known duration at various positions on the plate. The mean value of the solid angle was $\sim 5 \times 10^{-4}$ steradians for the slit settings used in these experiments.

TABLE 1. Isotopic Composition of the Yb Targets.

Target Mass	Isotopic Abundance						
	168	170	171	172	173	174	176
168	> 99	—	—	—	—	—	—
170	< 0.1	85.4	5.42	3.66	1.93	2.86	0.75
171	< 0.02	0.27	95.96	2.03	0.63	0.91	0.20
172	< 0.01	0.05	0.75	97.15	1.01	0.87	0.19
173	< 0.05	0.05	0.44	2.33	92.6	4.3	0.38
174	< 0.01	0.02	0.08	0.20	0.52	98.97	0.22
176	< 0.01	0.03	0.16	0.29	0.29	1.45	97.77

With a deuteron energy af 12 Mev and the mass differences encountered in this region of the periodic table, the ground-state triton group always had a greater magnetic rigidity than the elastic deuterons. The excitation energy in the triton spectrum, at which the elastic deuteron peak appeared, increased from ~1 Mev with a Yb168 target to ~3 Mev with a Yb176 target. The magnetic rigidity of the ground state proton group was always less than that of the elastic deuterons and therefore these groups appeared at an excitation of several Mev in the inelastic deuteron spectrum. For these experiments, an absorbing foil of aluminium, 27 mg/cm² thick, was placed over the region of the photographic plates where the deuterons were expected, in order to prevent tritons from appearing in the deuteron spectra. Aluminium foils from 100 mg/cm² to 154 mg/cm² thick were placed over the plates where the protons were expected in order to stop deuterons, tritons and alpha particles. These foils also served the purpose of reducing the proton energy such that the desired proton tracks were denser and thus easier to count. No absorbing foil was used over the plates where the triton groups were expected. The plate-holder was loaded with five photographic plates, 20.3 cm long×5.1 cm wide, placed end to end. The plates were manufactured by Ilford and had a Type K2 emulsion with a thickness of 25 microns. In this manner it was possible to record simultaneously the proton, triton and inelastic deuteron spectra from a target, although in practice some information from at least one of these spectra was often lost due to the cracks where the plates were joined.

Beam currents from 100 nA to 600 nA were used and the total charge for each exposure was measured with a Faraday cup and current integrator. In the analysis of the data, peak intensities were determined relative to the intensity of the elastic deuteron peak. However, on the long exposures required, the track density in the elastic peak was so great that counting was impossible. Therefore, a short exposure, planned to give a reasonable number of tracks in the elastic peak, was made immediately before and/or after the long exposure. The relative intensities of the short and long exposures were determined from the charges measured by the beam current integrator.

In order to convert these relative intensities into absolute cross sections for the proton and triton groups, separate experiments were performed to measure the absolute cross section for elastic deuteron scattering. Two separate approaches were tried. In one case, an Yb target was placed in a scattering chamber where a solid-state counter was used as a detector. The angular distribution of the elastic peak was measured for 12 Mev deuterons.
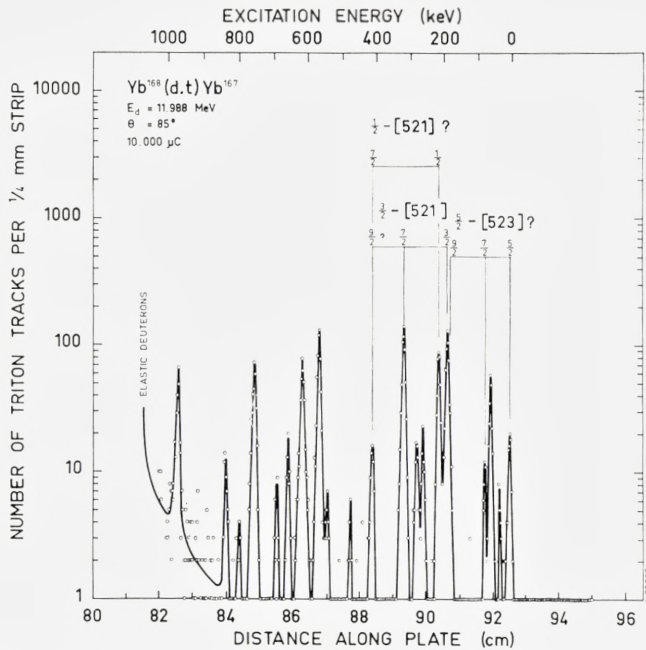
Figure 1. Triton spectrum for the reaction $Yb^{168}(d,t)Yb^{167}$ at $\theta = 85°$.

If one assumes that the cross section for small angle scattering approaches the Rutherford cross section, these data can be normalized to absolute values without a knowledge of target thickness, detector solid angle, etc. For the second method, the same experimental arrangement was used and the relative intensities of elastic deuterons were measured at several angles for beam energies of 5 Mev and 12 Mev. By assuming that the 5 Mev elastic scattering cross section is equal to the Rutherford cross section, the absolute value for the 12 Mev elastic scattering cross section is obtained. The two methods gave results which agreed within 10 %, and the estimated uncertainty in the results is ~15 %. This procedure was carried out for targets of several different Yb isotopes, but any differences in the elastic scattering cross sections for the different masses were smaller than the experimental uncertainties. Therefore, in the analysis of the data, the same elastic scattering cross section was assumed for all masses of ytterbium. The values used were 460 mb/sr, 60 mb/sr and 13 mb/sr for scattering angles of 60°, 90° and 125°, respectively. No attempt has been made to measure angular distributions of the reaction products. For most reactions, spectra have been obtained at two, and sometimes three, of the angles stated above, in

TABLE 2. Levels Populated in Yb[167].

Energy	Previously Known Energy	Nilsson Assignment	$d\sigma/d\Omega$ (d,t)*				
			$\theta = 56°$	$\theta = 60°$	$\theta = 85°$	$\theta = 90°$	$\theta = 125°$
0	0	5/2 5/2 − [523]	9	~ 5	13		
30			5	~ 4	~ 3		
59			15	17	34	28	
79		7/2 5/2 − [523]	~ 2	~ 3	7		
187		9/2 5/2 − [523] + 3/2 3/2 − [521]	49	45	90	96	78
212		1/2 1/2 − [521] ?	42	52	62	55	40
258			12	10	12	19	
277			4	6	12		
316		7/2 3/2 − [521]	50	64	98	124	89
408		9/2 3/2 − [521] + 7/2 1/2 − [521] ?	~ 7		12		~ 22
477					2		
545					~ 4		
566			~ 40	44	89	82	
601			~ 4				
614			~ 26	30	~ 60	62	
660				9	10		
692					~ 4		
752			~ 22	21	52	47	
801					~ 2		
835				5	~ 8	~ 10	
966				24	~ 33	28	

* Due to the fact that the areas of the Yb[168] targets were small, greater difficulties were encountered in normalizing intensities to the elastic scattering cross sections. Hence the uncertainties on relative values from different angles can be as great as 20%, as compared with 10% for the other Yb targets.

order to help isolate impurity peaks by means of their different kinematic shift of energy with angle.

The photographic plates were scanned by counting the tracks in strips, $1/4$ mm wide, using microscopes with specially constructed stages. For the determination of energies the peak positions were defined to be the positions of one-third maximum height on the high energy sides of the peaks. The calculation of output energies and Q-values was performed on a GIER digital computer. Energy calibration of the spectrograph was carried out using the 6.0498 Mev and 8.7864 Mev alpha particle groups from an active deposit of ThB placed in the target position.

The proton and triton spectra obtained for the different targets at $\theta = 90°$ are shown in Figures 1–10. For the case of the Yb[168] target, the spectra from
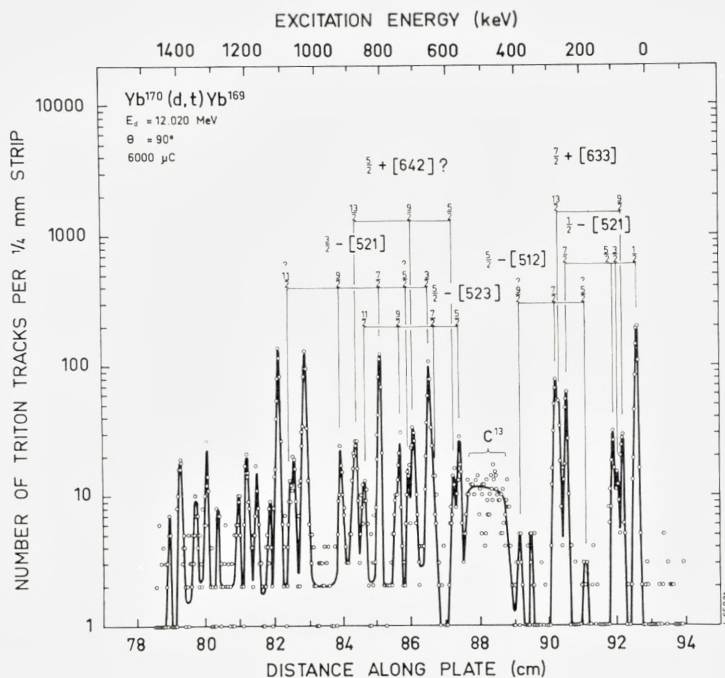
Figure 2. Triton spectrum for the reaction $Yb^{170}(d,t)Yb^{169}$ at $\theta = 90°$.

an experiment at $\theta = 85°$ are shown, because the reaction products from C^{13} in the target backing obscure important regions of the spectra at $\theta = 90°$. The excitation energies and cross sections for the various levels observed are given in Tables 2–7. The energies quoted in the first column of Tables 2–7 are the averages of the values obtained from the various exposures. The uncertainties in excitation energies are less than 2 or 3 kev for low-lying states and less than 5 or 6 kev for states at ~1.5 Mev excitation. The level assignments given in the third columns of these tables are discussed in the next section.

The cross sections in Tables 2–7 have been corrected for variation of the solid angle of the spectrograph with radius and for the contributions of isotopic impurities in the elastic peaks used for normalization. In the course of this work, a number of exposures have been repeated, and the intensities of the strong peaks were found to be reproducible to within 10 %. In view of this, and the possible variation in the elastic cross sections with mass, the uncertainty in relative intensities from different target masses is estimated to be not greater than ~15 %. The absolute intensities are also subject to

TABLE 3. Levels Populated in Yb^{169}.

Average (Weighted) Energy	Previously Known Energy	Nilsson Assignment	$\frac{d\sigma}{d\Omega}(d,t)\frac{\mu b}{sr}$		$\frac{d\sigma}{d\Omega}(d,p)\frac{\mu b}{sr}$		
			$\theta=60°$	$\theta=90°$	$\theta=56°$	$\theta=60°$	$\theta=85°$
0	0	7/2 7/2 + [633]		not seen	~ 1		
24	24	1/2 1/2 − [521]	162	155	238	~ 230	115
70	71	9/2 7/2 + [633]	12	22	~ 13		14
84	87	3/2 1/2 − [521]	} 30	8	63	C^{13}*	49
98	100	5/2 1/2 − [521]		26			
	157	11/2 7/2 + [633]					~ 1 ?
192	191.5	5/2 5/2 − [512]			Si^{28}*	8	4
244	244	7/2 1/2 − [521]	32	48	99		72
266	{ 265	9/2 1/2 − [521]	} 46	} 26	300	Si^{28}*	228
		13/2 7/2 + [633]					
277	278.5	7/2 5/2 − [512]		65			
390	388	9/2 5/2 − [512]			7	7	7
487	488	11/2 1/2 − [521]			3		4
523	522	11/2 5/2 − [512]			5	6	4
569	570.5	5/2 5/2 − [523]	} 9	20	5		4
584		5/2 5/2 + [642]		11			
647	647	7/2 5/2 − [523]	} 69	~ 13	53	43	~ 10
657		3/2 3/2 − [521]		80			~ 17
704		9/2 5/2 + [642]	} 23	30	9	~ 6	10
718		5/2 3/2 − [521]		~ 12		~ 9	
747	746	9/2 5/2 − [523]	6	~ 22	~ 6	9	11
805		7/2 3/2 − [521] + K = 1/2 γ-vib	56	100	43	42	36
849		3/2 1/2 γ-vib	~ 3	~ 15	236	178	145
	871	11/2 5/2 − [523]	} 8	31			
877		13/2 5/2 + [642]			~ 9	~ 6	~ 4
911		5/2 1/2 γ-vib			70	47	49
925		9/2 3/2 − [521] ?	6	22			
959					76	48	37
996		7/2 1/2 γ-vib			21	Si^{28}*	19
1030			55	110	19		
1064			} 6	17	~ 18	~ 14	
1074				8	~ 8	~ 14	
1106			54	105	44	23	
1134				8	8		

<p align="center">TABLE 3 (continued).</p>

Average (Weighted) Energy	Previously Known Energy	Nilsson Assignment	$\frac{d\sigma}{d\Omega}(d,t)\frac{\mu b}{sr}$		$\frac{d\sigma}{d\Omega}(d,p)\frac{\mu b}{sr}$		
			$\theta = 60°$	$\theta = 90°$	$\theta = 56°$	$\theta = 60°$	$\theta = 85°$
1170				~ 6	11		
1182					~ 2	10	
1198			~ 6	21	9		
1225				11	13	14	
1285				~ 9	173	120	
1317				18	~ 20	18	
1351				~ 14	171	111	
1395			~ 7	20	68	58	
~ 1421				5	~ 4	7	
1459				16	~ 61	29	
1473					~ 40	23	
1526					73	46	
1553					~ 88	56	
1567					~ 21		
1607					~ 50		
1640					238		
1688					334		
1733					~ 61		
1767					~ 150		

* This section of the plate was obscured by reactions from the element indicated.

the error in the determination of the elastic scattering cross section and thus may have an error as large as 20–25 %. The smaller peaks have larger errors, not only because of poorer statistics (in these experiments, a total count of 100 tracks usually corresponds to about 10–20 microbarns per steradian), but also because of the danger of an impurity peak being included in the count. In the present work, isotopic impurities are not a serious problem in this respect because the spectra of all the stable species of Yb have been measured. Thus, where necessary, the contribution to a spectrum from this source can be easily subtracted. The C^{13} in the carbon of the target backings often resulted in "peaks" in the spectra, as can be seen in several of the figures. The protons and tritons from this impurity are also easy to identify because they always occur at the same energy and the "peaks" are broader. The extra broadness is due to the fact that the energy of out-coming particles has a greater variation with angle for a light target nucleus

than for a heavy one. As the slit at the entrance to the magnetic field region of the spectrograph usually subtended an angle of several degrees at the target, an appreciable energy spread can result for a light target nucleus. It should also be noted that another difficulty arises with the data in Tables 2–7. It often happens that peaks are found in the (d,t) and (d,p) spectra corresponding to the same excitation energy within the uncertainty of the measurements. However, due to the high density of levels, there is a possibility that more than one level is present. Thus, although both (d,p) and (d,t) cross sections may be quoted for such a level, it may be that they correspond to two different "unresolved" states.

The ground-state Q-values for the reactions studied are given in Table 8. For completeness, the data from odd targets have also been included. Columns 4 and 5 show the neutron separation energies calculated from the (d,t) and (d,p) Q-values and the last column shows the neutron separation energies obtained from the tables of MATTAUCH et al.[16]. The uncertainty on the present Q-value measurements is of the order of 12 kev.

4. Interpretation of the Spectra

The predicted intensity for the various states in a rotational band based on a Nilsson state can be calculated from expression (6). As the quantities U^2 and V^2 are not well known initially, it is not easy to predict accurately the absolute cross sections for levels near the ground state. However, since the value of V^2 is the same for all members in a rotational band, the relative intensities of the states within the band are preserved.

Representative values of the quantity φ_l are shown in Figure 11, plotted in a manner which shows the dependence on l and the Q-value. These values have been obtained from a DWBA calculation of SATCHLER[17] who has used reasonable values of the optical-model parameters*). There is evidence[6] that the angular distributions and absolute values calculated for the (d,p) process agree with experiment, but no such tests of the (d,t) calculations have been made. Table 9 shows the predicted differential (d,t) cross sections for some of the Nilsson orbitals found in this mass

* Optical-model parameters used in the calculations were as follows:

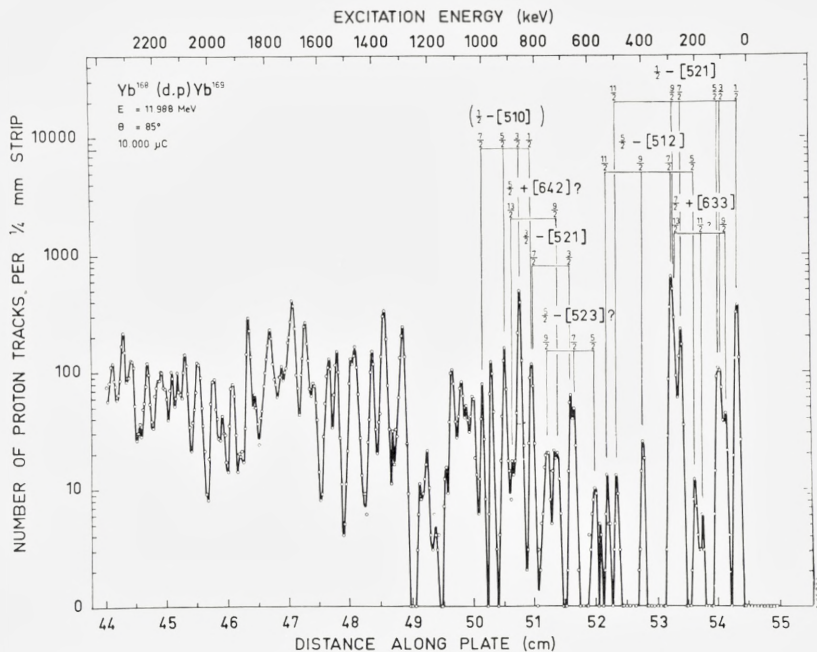|		V	W	r_0	a	r_0'	a'	W_D	r_c
(d,p)	Deuteron potential	86		1.15	0.87	1.37	0.7	12	1.25
	Proton potential	55		1.25	0.65	1.25	0.47	15	1.25
(d,t)	Deuteron potential	103	0	1.15	0.81	1.34	0.68	52	1.3
	Triton potential	100	14	1.07	0.854	1.7	0.73	0	1.4

Figure 3. Proton spectrum for the reaction $Yb^{168}(d,p)Yb^{169}$ at $\theta = 85°$.

region. These values were calculated using expression (6) with $\theta = 90°$, $Q = 0$, $V^2 = 1$. The C^2_{jl} were calculated from Nilsson's wave functions[1,6] for a deformation of $\eta = 6$, and the φ_l were obtained from Figure 11. The dependence of φ_l on the l-value for the (d,p) reaction is similar to that for the (d,t) reaction so the ratios of intensities within a band are not widely different in the two processes. (This is not true, of course, when the target nucleus is odd, where the simplified expression (6) is not valid.)

In the spectra of Figures 1–10 it is seen that many of the states corresponding to the observed proton and triton groups have been classified in terms of the Nilsson model. All the reasons for the choice of each assignment will not be discussed in detail. The decisions have been based largely on the fact that each Nilsson orbital has a characteristic distribution of intensity amongst the various members of its rotational band and that this distribution is similar for all nuclei. Other properties of the bands, such as moments of inertia, decoupling parameter (for $K = 1/2$ bands), systematics of excitation energy with neutron number, etc. were also considered. In the case of orbitals which originate from shell-model states of relatively small angular momenta, the members of the band with low spin values tend to have large

TABLE 4. Levels Populated in Yb[171].

Average (Weighted) Energy	Previously Known Energy	Nilsson Assignment	$\frac{d\sigma}{d\Omega}(d,t)\frac{\mu b}{sr}$		$\frac{d\sigma}{d\Omega}(d,p)\frac{\mu b}{sr}$	
			$\theta = 60°$	$\theta = 90°$	$\theta = 60°$	$\theta = 90°$
0	0	1/2 1/2 − [521]	480	340	167	68
72	{ 66.73	3/2 1/2 − [521]	} 95	82	42	34
	{ 75.88	5/2 1/2 − [521]				
121	122.4	5/2 5/2 − [512]		4.3	~ 14	~ 7.4
168	167.6	9/2 7/2 + [633]	28	38	12	10.3
208	208.0	7/2 5/2 − [512]	115	127	208	160
230	230.5	7/2 1/2 − [521]	} 103	110	} 66	} 45
~ 250	247	9/2 1/2 − [521]		~ 11		
318	317.3	9/2 5/2 − [512] + Yb[172]		4.4	~ 6**	~ 6**
369		13/2 7/2 + [633]	18	48	11	25
449		11/2 5/2 − [512]		2.8	~ 8	~ 4.8
486		11/2 1/2 − [521]		4.6	~ 2.5	~ 5.3
838	835.0	7/2 7/2 − [514] + ?	14	22	51	38
~ 867	862		} 16		~ 3	~ 4
876						
902		3/2 3/2 − [521]*	104	117		
906					21	~ 12
945	948.3	9/2 7/2 − [514] + 1/2 1/2 − [510]*			44	50
971			} ~ 42	72		
~ 987						
995		3/2 1/2 − [510]*			298	198
1026			} ~ 46	62	32	~ 34
~ 1038						
1052		5/2 1/2 − [510]*			71	86
1079		7/2 3/2 − [521]*	~ 46	78	18	26
~ 1113					~ 4	~ 5
1118			~ 17	36		
1144		7/2 1/2 − [510]*			30	31
1188			~ 8	14		
1204					8	21
~ 1244				1		
1254		9/2 1/2 − [510]*			~ 6	9
1280				11		
1290					~ 31	~ 21
~ 1300				~ 6		
1320				15		
1328					144	93
1348			~ 41	72		

(continued)

TABLE 4 (continued).

Average (Weighted) Energy	Previously Known Energy	Nilsson Assignment	$\frac{d\sigma}{d\Omega}(d,t)\frac{\mu b}{sr}$		$\frac{d\sigma}{d\Omega}(d,p)\frac{\mu b}{sr}$	
			$\theta = 60°$	$\theta = 90°$	$\theta = 60°$	$\theta = 90°$
~ 1356					~ 28	~ 28
1387				~ 4		
1395					208	141
1402				~ 5		
1432				20	~ 36	~ 29
1460				27		
1486				28	250	175
1518			72	125		
1524					75	45
1559				~ 2		
1588					~ 23	32
1599				8		
1627					292	141
1638				20		
1662				19		
1671					358	174
1715				5		
1730					210	
1765					68	
1771				32		

* These states are thought to be γ-vibrations which contain large fractions of the single-particle states indicated. See text.

** After subtraction of ~ 6 $\mu b/sr$ due to isotopic impurity in the target.

values of C_{jl}^2 and thus strong cross sections. In these cases it is easy to make an unambiguous assignment of the observed peaks. However, orbitals originating from shell-model states of high angular momentum tend to have large values of C_{jl}^2 for the high spin states only. As the cross section decreases rapidly with increasing l-value, the net result is that the total population of such bands is more than an order of magnitude weaker than for the strongest ones. This situation is found in the present work for some of the Nilsson orbitals which come from the $i_{13/2}$ shell-model state. In addition, these bands usually have only about two states for which C_{jl}^2 is not vanishingly small, and hence only two members of the band are populated strongly enough to be observed. This makes the identification less certain than when several members are populated, especially if one of the two weak peaks is obscured by stronger groups.
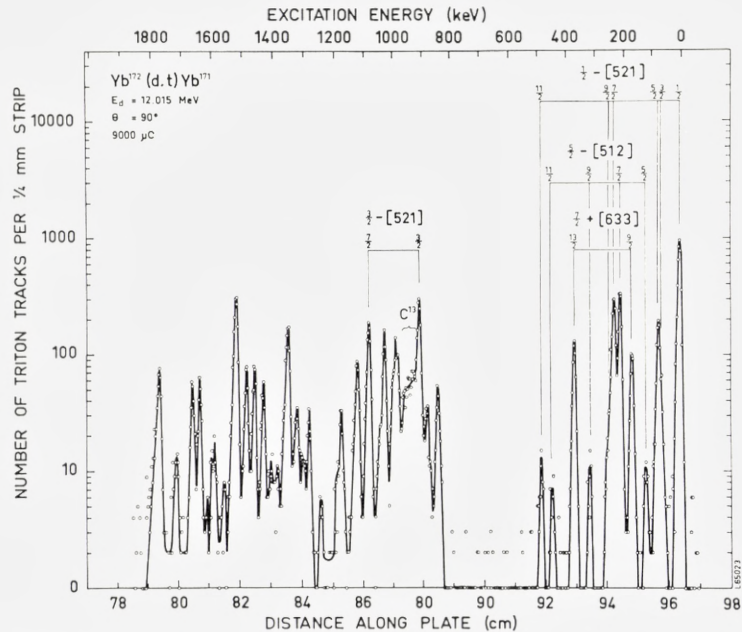
Figure 4. Triton spectrum for the reaction $Yb^{172}(d,t)Yb^{171}$ at $\theta = 90°$.

Level schemes for the Yb^{167}, Yb^{169}, Yb^{171}, Yb^{173} and Yb^{175} are given in Figures 12–16 where the assigned states are separated into rotational bands. No level scheme is given for Yb^{177} as the results are essentially the same as those of Vergnes and Sheline[6]. The excitation energy of the band head of each Nilsson state is shown plotted against the neutron number in Figure 17. Points plotted at negative energies in this diagram indicate that the orbital is a hole state, as determined from relative (d,p) and (d,t) cross sections and systematics.

In view of the similarity of the spectrum of a given band in one nucleus to that of the same band in the other nuclei, it seems reasonable to consider one orbital at a time, discussing its properties in the different isotopes. The bands which have the largest cross sections will be considered first.

A – The 1/2–[521]* Orbital

This orbital is known to be the ground state of Yb^{171} and it has a characteristic level spacing due to its decoupling parameter $a \approx 0.87$**. It occurs at an excitation energy of 24 kev in Yb^{169} and a similar level spacing is

---

* The notation used here is $K\pi[Nn_z\Lambda]$. When a particular member in a rotational band is referred to, the quantum numbers used are $IK\pi[Nn_z\Lambda]$.

** For previously known levels, see references 18–20.

TABLE 5. Levels Populated in Yb[173].

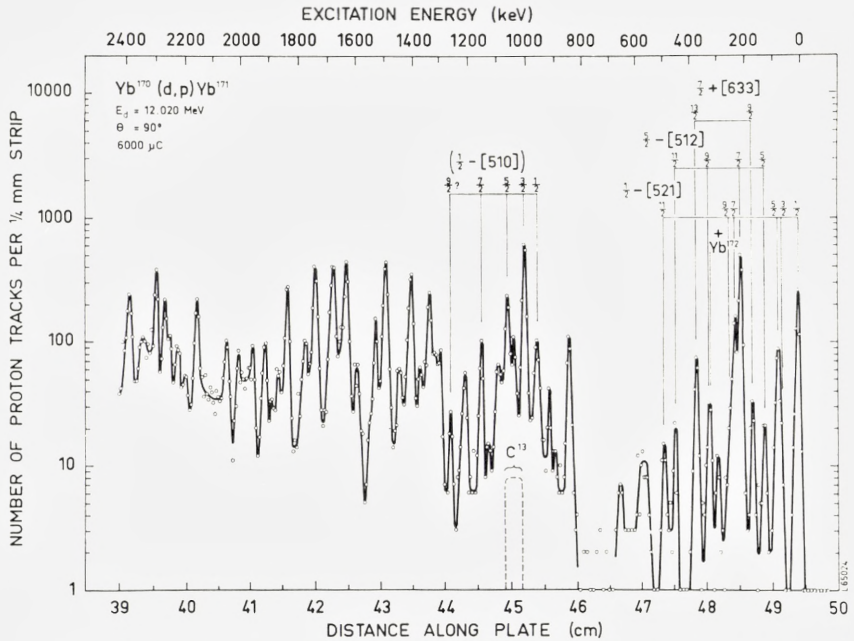| Average (Weighted) Energy	Previously Known Energy	Nilsson Assignment	$\frac{d\sigma}{d\Omega}(d,t)\frac{\mu b}{sr}$		$\frac{d\sigma}{d\Omega}(d,p)\frac{\mu b}{sr}$	
			$\theta = 60°$	$\theta = 90°$	$\theta = 90°$	$\theta = 125°$
0	0	5/2 5/2 − [512]	19	20	8	~ 2
79	78.7	7/2 5/2 − [512]	440	450	165	64
179	179.6	9/2 5/2 − [512]	~ 3	1	7	4
301		11/2 5/2 − [512]	~ 4	12	~ 7	4
398	399	1/2 1/2 − [521]	}630	475	54	15
~ 410	413.3	9/2 7/2 + [633]				
~ 462		3/2 1/2 − [521]	}120	30	9	~ 5
478		5/2 1/2 − [521]		80	15	
600		13/2 7/2 + [633] + ?	~ 25	58	35	~ 15
620		7/2 1/2 − [521] + ?	}109	130	}63	21
630	636	7/2 7/2 − [514] + ?				
655		9/2 1/2 − [521]	~ 3	12		
743		9/2 7/2 − [514]	~ 2	9	45	12
875		11/2 1/2 − [521]		8		
890					~ 9	4
1031		1/2 1/2 − [510]			~ 12	~ 2
1073		3/2 1/2 − [510]	11	19	370	145
1120		5/2 1/2 − [510]	5	12	190	76
1168			3	26	~ 4	
1221		7/2 1/2 − [510]			93	40
1224		3/2 3/2 − [521]	94	112		
1306		9/2 1/2 − [510]			16	~ 15
1324			12	12		
1340		3/2 3/2 − [512]			127	36
1354		7/2 3/2 − [521]	60	88		
1404		5/2 3/2 − [512]	5	9.6	209	78
1440			28	58		
1445					~ 15	
1496		7/2 3/2 − [512]			114	41
1582			17	27		
1605		9/2 3/2 − [512] + ?		18	22	~ 28
1625				17		
1665				11	430	168
1714			5	24	252	130
1735				12	112	~ 50
1765			~ 2	~ 25	78	~ 48
1790					99	
1815				14		
1855				170		
1878				45		

Figure 5. Proton spectrum for the reaction $Yb^{170}(d,p)Yb^{171}$ at $\theta = 90°$.

observed. The first two members of the band have also been found in Yb^{173} where the band head energy is 399 kev[21].

From Table 9 it appears that all states up to a spin of 11/2 should be populated in the present work. This is seen to be the case in Yb^{171} where, however, the 3/2 and 5/2 states are not resolved from each other and the peak due to the 9/2 level shows as a shoulder on the side of that due to the 7/2 state. The level energies are in good agreement with those previously reported. The 11/2 member had not been observed before, but its energy fits nicely into the sequence.

A similar intensity pattern is found in Yb^{169} except that some of the weaker groups were not seen. The 3/2 and 5/2 states are resolved in the (d,t) spectrum but the group due to the 9/2 level is hidden by a larger peak. That of the 11/2 state is obscured by the C^{13} "peak" in Figure 2, but can be seen in Figure 3. It is noted that the ground state of Yb^{169} is the 7/2 + [633] orbital. As the 7/2 member of this band has an extremely small value of C^2_{jl} it is not seen in this work. Hence, the 1/2 1/2−[521] state at 24 kev excitation is the first level for which a triton or proton group is actually seen. For all levels in Yb^{169}, energies have been measured relative to the

Table 6. Levels Populated in Yb[175].

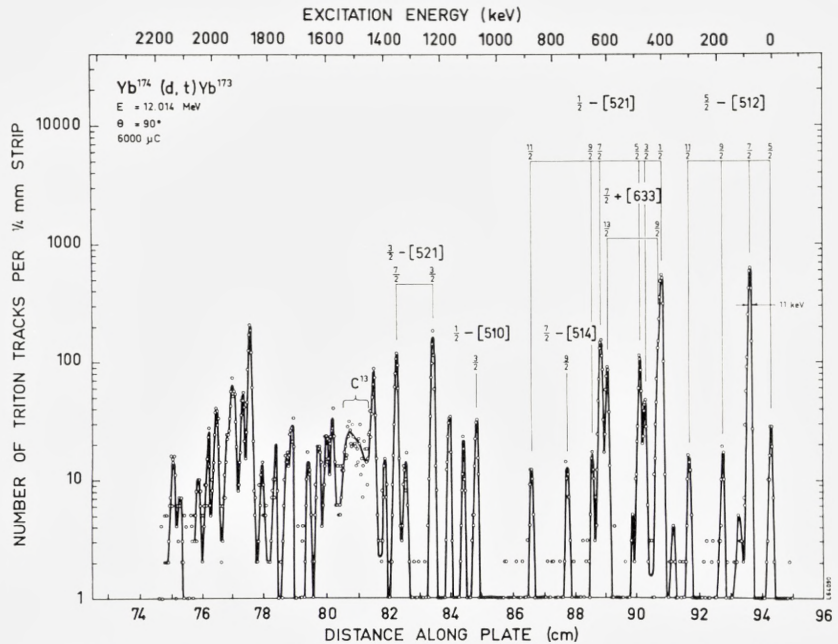| Average (Weighted) Energy	Previously Known Energy	Nilsson Assignment	$\frac{d\sigma}{d\Omega}(d,t)\frac{\mu b}{sr}$ $\theta=60°$	$\frac{d\sigma}{d\Omega}(d,t)\frac{\mu b}{sr}$ $\theta=90°$	$\frac{d\sigma}{d\Omega}(d,p)\frac{\mu b}{sr}$ $\theta=90°$	$\frac{d\sigma}{d\Omega}(d,p)\frac{\mu b}{sr}$ $\theta=125°$
0	0	7/2 7/2−[514]	14	13	~ 15	~ 3
101		9/2 7/2−[514]	43	59	~ 35	15
225		11/2 7/2−[514]		~ 3		
260		9/2 9/2+[624]		12		
511*		1/2 1/2−[510]	}30	50	64	30
516		13/2 9/2+[624]				
552		3/2 1/2−[510]	120	84	390	105
600		5/2 1/2−[510]	43	45	176	56
633		5/2 5/2−[512]	< 34	~ 26	~ 7	~ 4
694		7/2 1/2−[510]	< 12	~ 11	79	29
723		7/2 5/2−[512]	540	500	93	29
773		9/2 1/2−[510] + ?		~ 3	22	11
809		3/2 3/2−[512]	18	14	106	24
837		9/2 5/2−[512]		~ 7		
868		5/2 3/2−[512]	48	35	233	82
913		1/2 1/2−[521]	630	400	~ 22	~ 7
954		7/2 3/2−[512]	~ 10	16	115	33
~ 977		11/2 5/2−[512]	}125	~ 12		
~ 984		3/2 1/2−[521]		~ 26		
1004		5/2 1/2−[521]		86	~ 7	
1061		9/2 3/2−[512] + ?	~ 8	~ 8	~ 20	~ 3
1088		9/2 7/2+[633] + ?	~ 45	42	~ 17	
1166		7/2 1/2−[521]	108	108		
1196		9/2 1/2−[521]	~ 5	~ 14		
1300			~ 6	~ 10	~ 9	
1336		13/2 7/2+[633]	}25	38		
1360				~ 10	755	215
1420			~ 8	~ 8	377	147
1460		11/2 1/2−[521] + ?		~ 5	228	77
1616		3/2 3/2−[521]	104	90		13
1677		5/2 3/2−[521]	20	22		
1745			~ 5	~ 8		
1765		7/2 3/2−[521]	54	71		

* Energy estimated from level spacings of other members of this band.

Figure 6. Triton spectrum for the reaction $Yb^{174}(d,t)Yb^{173}$ at $\theta = 90°$.

1/2 1/2−[521] group and then increased by 24 kev to yield excitation energies above the ground state.

In Yb^{173} and Yb^{175}, all six members of this band are clearly seen in the (d,t) process. A comparison of the observed relative (d,t) intensities with predicted values is given in Table 10. For each nucleus, there are two columns. The left shows the relative cross section at $\theta = 90°$ normalized to 100 for the 1/2 1/2−[521] state. The right column shows the values of C_{jl}^2 obtained from the relative intensities, using values of φ_l from Figure 11. The values of C_{lj}^2 given have been normalized such that their sum is equal to unity. For the case of Yb^{169} it was not possible to normalize in this manner as two of the weak peaks were not seen. In this case, the value of C_{jl}^2 for the spin 1/2 member was set equal to that of the same state in Yb^{171}.

Values for the decoupling parameter and inertial parameter, $\hbar^2/2\mathfrak{J}$, obtained from the energy spacings of the levels, are given in Table 11 where the data for all bands are summarized. The observed dependence of these quantities on the neutron number for the 1/2−[521] orbital fits quite well into a plot such as that given by SHELINE et al.[22].

TABLE 7. Levels Populated in Yb[177].

Average Energy	Previously Known Energy	Nilsson Assignment	$\frac{d\sigma}{d\Omega}(d,p)\frac{\mu b}{sr}$	
			$\theta = 90°$	$\theta = 125°$
0	0	9/2 9/2+[624]	Obscured	~ 1
111	109	7/2 7/2−[514]	~ 2	
124	123		~ 1	
222	220	9/2 7/2−[514]	12	5
268	265	13/2 9/2+[624]	35	15
306	306	Yb[174] impurity	6	~ 1
335	333	1/2 1/2−[510]	9	
379	379	3/2 1/2−[510]	305	89
424	426	5/2 1/2−[510]	148	46
530	527	7/2 1/2−[510]	59	26
615	614	9/2 1/2−[510]	14	8
708	709	3/2 3/2−[512]	168	51
774	773	5/2 3/2−[512]	218	68
822			~ 14	
867	868	7/2 3/2−[512]	112	33
976	976	9/2 3/2−[512]	15	9
1050			7	
1104			11	
1124			5	
1173			5	
1222	1226	7/2 7/2−[503]	346	121
1362	1365	3/2 3/2−[501]	740	235
1447	1449	5/2 3/2−[501]	172	
1496			70	
1564	1567	7/2 3/2−[501]	14	

The absolute intensities of the triton and proton groups are dependent on V^2, the probability that the state is filled in the target nucleus. In Figure 18, the (d,p) and (d,t) cross sections for the 1/2 1/2−[521] state at $\theta = 90°$ are shown as a function of target mass. As the absolute cross section is dependent on the Q-value, the (d,t) data have all been adjusted to the corresponding values for $Q = -1.5$ Mev with the aid of the Q-value dependence from Figure 11. Similarly, the (d,p) cross sections have been corrected to the values they would be for $Q = 4.0$ Mev. The data are interpreted as being an indication of the filling of the 1/2−[521] state in the various isotopes. In the heavier targets, the (d,p) cross section becomes small and the (d,t) cross section tends to become constant. This means that the state is nearly
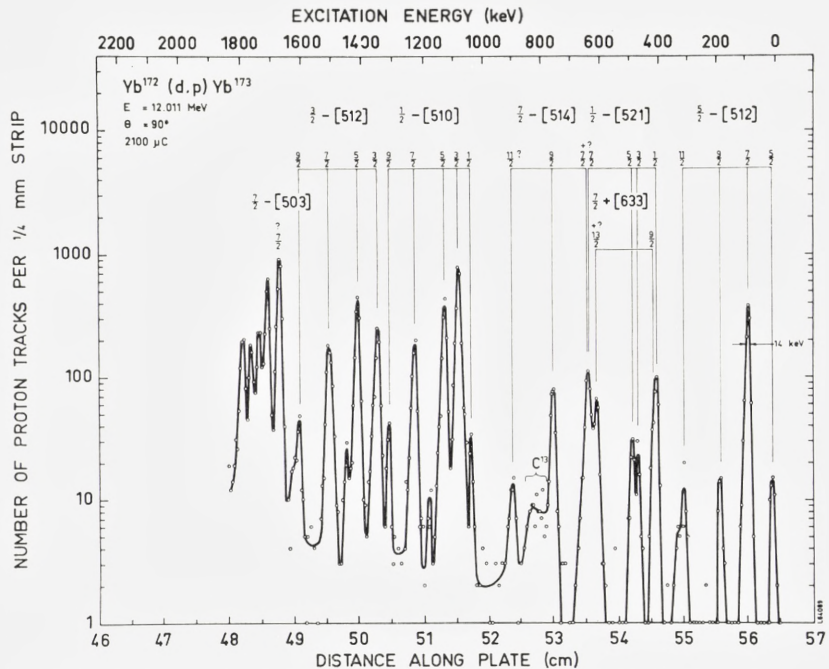
Figure 7. Proton spectrum for the reaction $Yb^{172}(d,p)Yb^{173}$ at $\theta = 90°$.

filled in these isotopes, as would be expected since it is the ground state of Yb^{171}. Below mass 171, the cross section for (d,t) becomes small, while that for (d,p) is large, indicating that the state is nearly empty.

B – *The 5/2–[512] Orbital*

This orbital originates from a $2f7/2$ shell-model state and the $7/2$ member is the only one which has a large value of C_{jl}^2. Thus, the $7/2$ state is predicted to be strongly populated while the $5/2$, $9/2$ and $11/2$ levels are not. This distribution among the four states is seen experimentally by the (d,p) and (d,t) processes in Yb^{173} where this orbital appears as the ground state. Peaks due to all four members of this band can also be seen in the proton spectra of Yb^{171} and Yb^{169}, and in the triton spectra of Yb^{175} and Yb^{171}. In the remaining spectra some of the weaker peaks are too small to be observed. Table 12 shows a comparison of the predicted relative intensities and C_{jl}^2 values with those determined experimentally. Figure 18 shows a plot of the (d,p) and (d,t) cross sections for the $7/2$ $5/2–[512]$ state at $\theta = 90°$ as a function of mass number. The Q-value dependence

TABLE 8. Neutron Separation Energies for Yb Nuclei.

Mass A	$Q(d,t)$ A → A − 1 Mev	$Q(d,p)$ A − 1 → A Mev	$S_n(A)$ from $Q(d,t)$ Mev	$S_n(A)$ from $Q(d,p)$ Mev	$S_n(A)$ from Mass Tables[16] Mev
168	− 2.797 ± 0.012	—	9.055 ± 0.012	—	8.980 ± 1.010
169	—	4.636 ± 0.012	—	6.861 ± 0.012	6.790 ± 1.010
170	− 2.211 ± 0.012	—	8.469 ± 0.012	—	8.550 ± 1.000
171	− 0.359 ± 0.012	4.390 ± 0.012	6.617 ± 0.012	6.615 ± 0.012	6.760 ± 0.070
172	− 1.772 ± 0.012	5.797 ± 0.012	8.030 ± 0.012	8.022 ± 0.012	8.140 ± 0.080
173	− 0.114 ± 0.012	4.145 ± 0.012	6.372 ± 0.012	6.370 ± 0.012	6.480 ± 0.060
174	− 1.218 ± 0.012	5.239 ± 0.012	7.476 ± 0.012	7.464 ± 0.012	7.440 ± 0.070
175	—	3.595 ± 0.012	—	5.820 ± 0.012	5.840 ± 0.080
176	− 0.621 ± 0.012	—	6.879 ± 0.012	—	6.640 ± 0.080
177	—	3.337 ± 0.012	—	5.562 ± 0.012	5.530 ± 0.110

has been removed from these values as for the 1/2 1/2−[521] case. It is seen that this orbital appears to be half-filled at a neutron number two units greater than for the 1/2−[521] state. This is reasonable as it is the ground state of Yb[173], which is two units heavier than Yb[171].

For several cases where the above two orbitals were hole states, identification of the weak peaks in the proton spectra was possible only because the excitation energies of the levels were known from assignments made on the basis of the triton spectra. This is one of the advantages of using the two complementary reaction processes in conjunction with each other for such studies.

C − The 1/2−[510] Orbital

The 1/2−[510] orbital has been found previously[6] in a study of Yb[177] levels by means of the (d,p) reaction. It is characterized by large cross sections to several members of the band, an inertial parameter of $\hbar^2/2\mathfrak{J} = 12.2$ kev and a decoupling parameter $a = 0.22$. This band is also seen in Figure 10 of the present work. Anomalous rotational bands with similar intensity patterns are also found in the proton spectra of Yb[175] and Yb[173] and have been assigned to the 1/2−[510] orbital. The spin 1/2 member of this band is populated rather weakly and in Yb[175] is not resolved from the larger 13/2 9/2 + [624] peak. Relative intensities and relative values of C_{jl}^2 for the various states observed in this band in Yb[177], Yb[175] and Yb[173] are shown in Table 13, where the theoretical values are included for comparison. As the 11/2 state was not observed, its value of C_{jl}^2 cannot be determined.

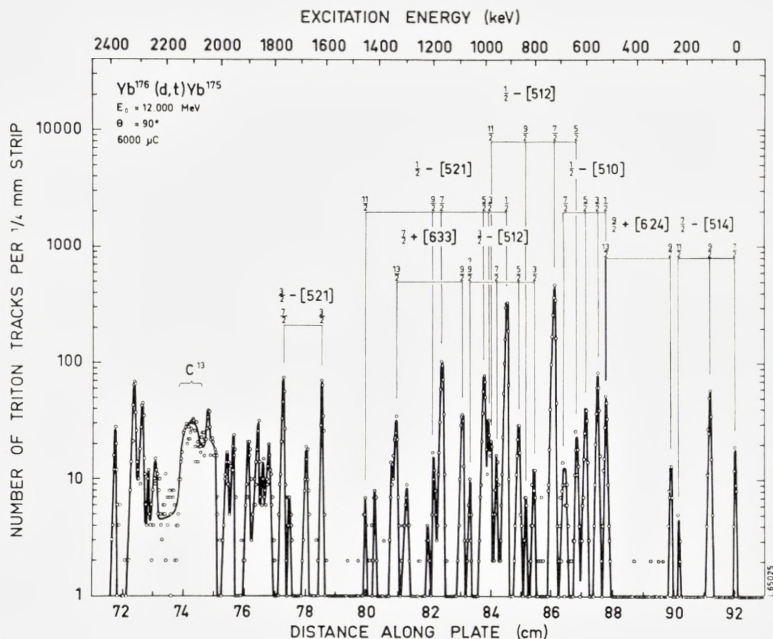Figure 8. Triton spectrum for the reaction $Yb^{176}(d,t)Yb^{175}$ at $\theta = 90°$.

In Yb^{173} and Yb^{175}, an upper limit of ~ 0.15 can be given for the C_{jl}^2 of this state. From Table 13 it is seen that this quantity is expected to be very small and thus the values of C_{jl}^2 are normalized such that those of the observed states add to unity. This normalization should not be more than 15 % different from that which would have been obtained if all the members of the band had been observed.

Although this band would be expected to have an excitation energy slightly greater than one Mev in Yb^{171}, there is no peak in Figure 5 below two and one-half Mev excitation which has a cross section as large as that expected for the 3/2 1/2−[510] state. The most intense peak in the region of 1 Mev appears to be the spin 3/2 member of a $K = 1/2$ band which has an intensity distribution among the various spin members similar to that of the 1/2−[510] orbital. However, the absolute intensities are only about 60 % of what would be expected for this orbital on the basis of the intensities in Yb^{173} and Yb^{175}, after making allowance for the difference in Q-value. The decoupling parameter is also smaller than in the heavier Yb isotopes (see Table 11). This behaviour is ascribed to mixing between the single-particle states and vibrational states and will be discussed in a later section.
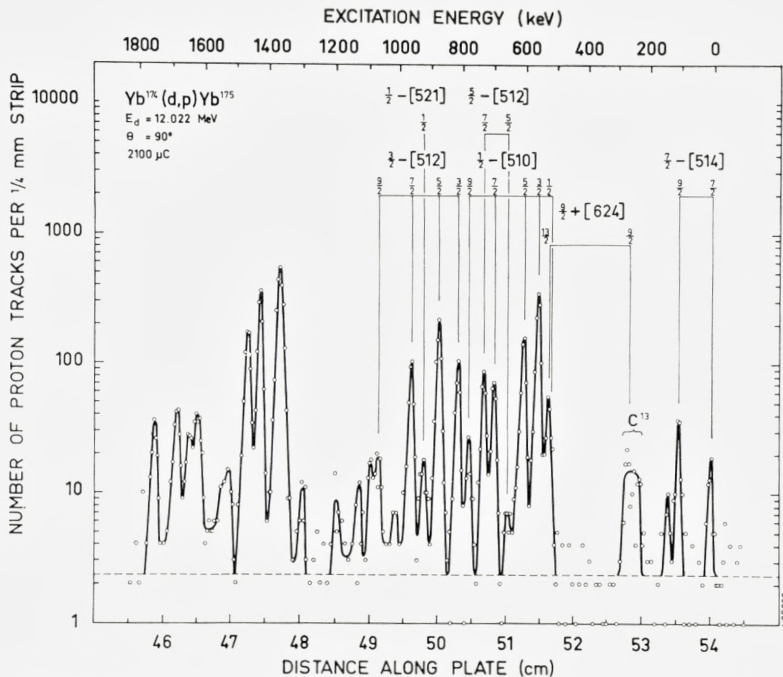
Figure 9. Proton spectrum for the reaction $Yb^{174}(d,p)Yb^{175}$ at $\theta = 90°$.

The relative intensities of states in this band have been included in Table 13 to show how the intensity pattern resembles that of the $1/2-[510]$ band.

A similar phenomenon appears to take place in the Yb^{169} spectrum of Figure 3, except that in this case two bands with relative intensities similar to those of the $1/2-[510]$ orbital are found. The absolute intensities of these are about 40% and 45% of that which would be expected for the pure band. It is clear that this behaviour is more complicated than that seen for the same orbital in Yb^{173}, Yb^{175} and Yb^{177} and for the $1/2-[521]$ and $5/2-[512]$ orbitals discussed above. Consequently, the interpretation is more difficult and less certain. The variation of the cross section of the strongly populated $3/2$ $1/2-[510]$ state with target mass is shown in Figure 19. As this orbital should be the ground state of Yb^{179}, comparison with Figure 18 shows that the (d,p) cross section into Yb^{177} is less than that into Yb^{173} and Yb^{175} because the U^2 is smaller. The weaker bands mentioned above are also included in this diagram.

The $1/2-[510]$ orbital provides a sensitive means for assessing the importance of the two-step process of rotational excitation and stripping. The
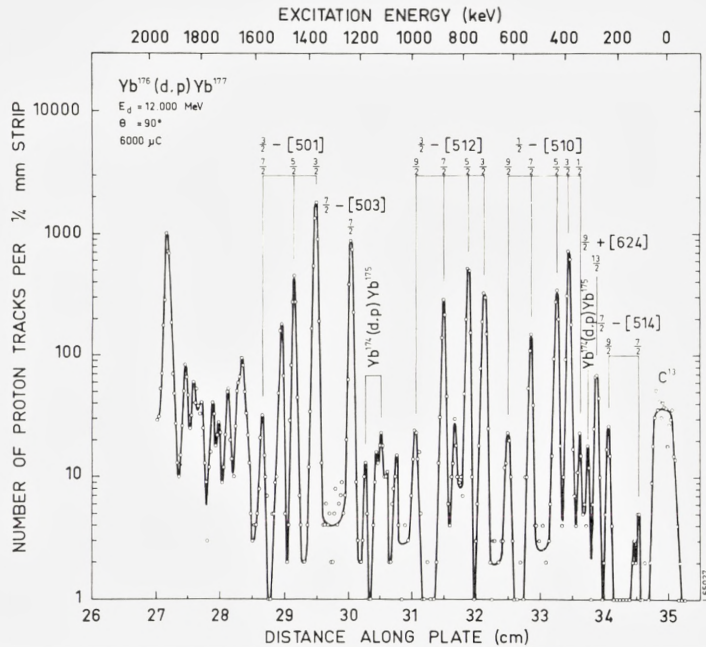
Figure 10. Proton spectrum for the reaction Yb$^{176}(d,p)$Yb^{177} at $\theta = 90°$.

theoretical spectroscopic factor for the 3/2 member is 40 times that of the 1/2 member for the direct process. With rotational excitation and stripping, the strong $j = 3/2$ transition may contribute to formation of the 1/2 state. An enhancement of the 1/2 cross section by maybe a factor of 3 is obtained from a qualitative estimate based upon the cross section for inelastic deuteron scattering to the 2+ state. The measured spectroscopic factor for the 1/2 state relative to that of the 3/2 state is only about 30 % to 50 % larger than theoretically calculated and, in fact, constitutes excellent agreement for a state with such a small spectroscopic factor. Since we do not observe a contribution from rotational excitation and stripping in a particularly favourable reaction where even a small admixture would have easily observable effects, we conclude that it is reasonable to disregard the process. A similar conclusion has recently been reached for (d, p) reactions on W isotopes.[7]

D – The 3/2–[512] *Orbital*

This is another strongly populated band which has been classified[6] in Yb^{177}. In the present study, similar patterns of strong peaks have also been
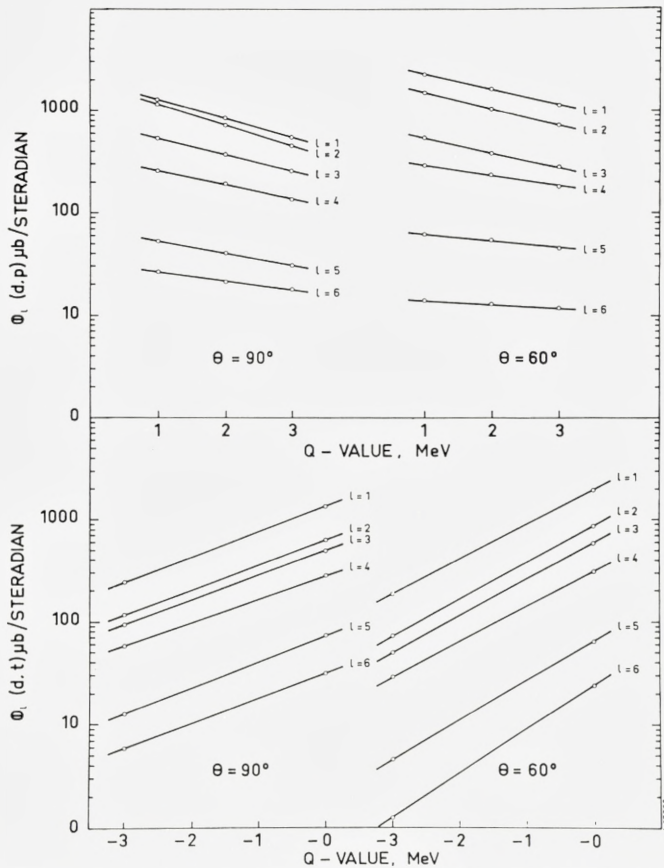
Figure 11. Typical values of the single-particle cross sections φ_l, obtained by SATCHLER[17]) who has performed a DWBA calculation with reasonable values for the optical parameters. The points in this figure are calculated values and the solid lines show the interpolation used in the present work. The (d,t) values given in the lower part of the figure are by mistake too high by a factor of 1.5.

found in the proton spectra of Yb^{173} and Yb^{175} and assigned to this orbital. The relative intensities at $\theta = 90°$ and relative values of C_{jl}^2 for these three nuclei are shown in Table 14 where also theoretical values are given. Again the proton group corresponding to the spin 11/2 state was too weak to be seen, and thus the values of C_{jl}^2 are normalized such that the sum for the observed states is unity.

The discrepancies between experiment and theory are greater for this orbital than for the ones discussed above. In all cases, the 7/2 and 9/2 states are more strongly populated relative to the 5/2 state than was predicted.
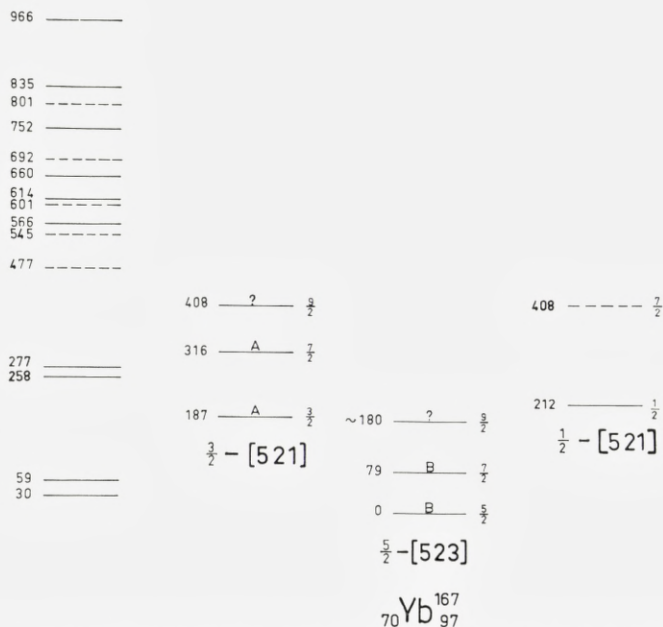
Figure 12. Level scheme for Yb[167]. Levels shown as dashed lines were populated very weakly and may possibly be due to heavy impurities. For the meaning of A and B, see caption to Figure 13.

However, in the absence of any other similar band of comparable absolute intensity, there is no doubt as to the certainty of the assignment.

The strong peaks of both the $1/2-[510]$ and $3/2-[512]$ orbitals can also be seen weakly in the triton spectra of Yb[173] and Yb[175]. Needless to say, many of these peaks would not have been identified if the assignments made on the basis of the proton spectra had not been available.

E – The $7/2+[633]$ Orbital

From Table 9 it is seen that only the 9/2 and 13/2 spin members of this band are expected to be populated strongly enough to be detected in the present work. This is found to be the case in the nuclei where the orbital has been observed.

As the excitation energies of several members of this band were previously known in Yb[169], Yb[171] and Yb[173], identification was no problem in these nuclei. The assignment of the states in Yb[175] at 1088 kev and 1336 kev to the 9/2 and 13/2 spin members of this band is based mainly on the fact that these are the only two unexplained hole states with reasonable cross
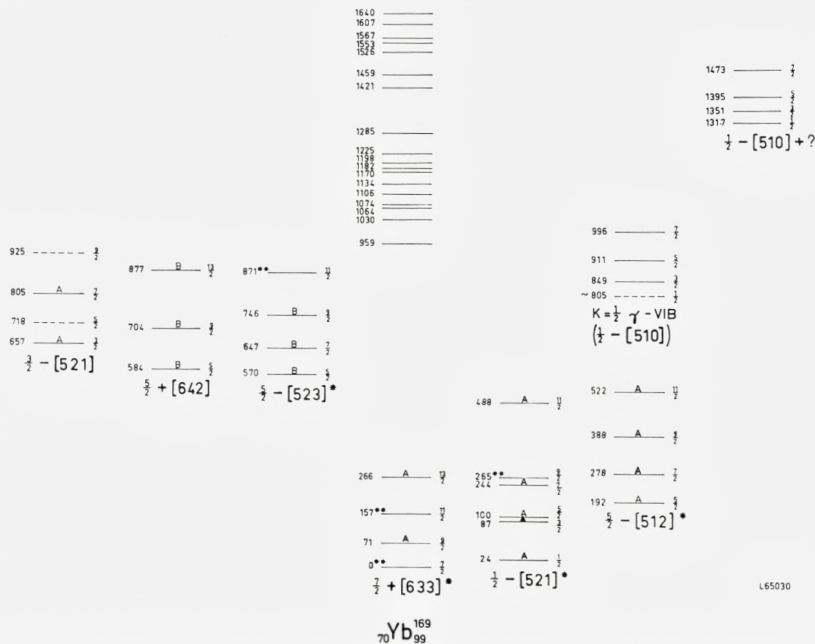
Figure 13. Level scheme for Yb[169]. For bands labelled with an asterisk, the more precise level energies from reference 23) are shown. Individual states with two asterisks were populated too weakly to be observed, or were obscured by larger peaks, in the present work. Letter A indicates a high degree of certainty in the assignment given to a level. Letter B means that the available data suggest the quantum numbers shown, but due to the fact that the peaks are relatively weak, the assignment is considered to be somewhat tentative. For vibrational states refer to the text.

sections in the region of excitation energy where this orbital is expected to be found.

The relative intensities and relative values of C_{jl}^2 for the 9/2 and 13/2 members of this band, populated in the (d,t) process in Yb[169], Yb[171] and Yb[175], are shown in Table 15 where they are compared with predicted values. Data for Yb[173] are not shown because the triton group due to the 9/2 state is not resolved from the strong 1/2 1/2−[521] group. The agreement with predictions is quite good.

F − *The 7/2−[514] Orbital*

The position of this orbital was also known previously for Yb[177], Yb[175], Yb[173] and Yb[171]. As the C_{jl}^2 is large only for the spin 9/2 state, which has $l = 5$, there are no strongly populated levels in the band. However, the intensities of the proton groups in Yb[173], Yb[175] and Yb[177], as well as the triton groups

TABLE 9. Predicted Cross-Sections for (d, t) Reactions $Q = 0$ $\theta = 90°$ $V^2 = 1$.

Orbital/Spin	1/2	3/2	5/2	7/2	9/2	11/2	13/2
3/2 + [402]	–	710	58	27	2	–	–
1/2 + [400]	1090	200	94	14	2	–	–
9/2 – [514]	–	–	–	–	1	88	–
11/2 – [505]	–	–	–	–	–	90	–
1/2 – [541]	196	250	190	26	25	13	–
1/2 – [530]	11	384	39	153	31	13	–
3/2 – [532]	–	69	140	54	51	10	–
1/2 + [660]	10	2.2	45	0.9	94	0.08	28
3/2 + [651]	–	0.7	18	1.8	75	0.4	32
3/2 – [521]	–	188	~ 0	342	23	10	–
5/2 + [642]	–	–	3.6	1.2	49	0.54	35
5/2 – [523]	–	–	49	50	71	5.4	–
1/2 – [521]	448	44	120	153	24	4.1	–
7/2 + [633]	–	–	–	0.3	25	0.62	38
5/2 –]512]	–	–	6.6	520	13	5.6	–
7/2 – [503]	–	–	–	610	5	1.9	–
7/2 – [514]	–	–	–	28	83	2.6	–
9/2 + [624]	–	–	–	–	8	0.54	40
1/2 – [510]	18	730	192	125	8	1.3	–
3/2 – [512]	–	144	420	77	13	0.11	–
3/2 – [501]	–	1380	93	50	1	~ 0	–

in Yb[175], are in agreement with the predicted values and can be considered to be verifications of the assignments. In Yb[171] the spectra are quite complicated in the energy region where this orbital has previously been assigned. The data are consistent with this assignment but cannot be considered as a definite verification.

G – The 9/2 + [624] Orbital

Table 9 shows that none of the rotational members in this band should be strongly populated. Hence, in the present work it can be identified only in Yb[177] where it is the ground-state band, and in Yb[175] where it appears at 260 kev excitation with no other strongly populated states to interfere. It is not surprising that it cannot be found in Yb[173] because there are many strong groups which could obscure the weak peaks.

H – The 3/2 – [521] Orbital

From Table 9 it is seen that this band should be characterized by strongly populated 3/2 and 7/2 states with only weak transitions to the other

TABLE 10. (d,t) Population of $1/2-[521]$ Band.

Spin	Relative Intensity $\theta = 90°$					Values of C^2_{jl}				
	Theory	Yb^{169}	Yb^{171}	Yb^{173}	Yb^{175}	Theory	Yb^{169}	Yb^{171}	Yb^{173}	Yb^{175}
1/2	100	100	100	100	100	0.249	0.284*	0.284	0.300	0.282
3/2	9.3	~ 5.2	} 24	6.3	6.5	0.024	0.015*	0.018**	0.020	0.019
5/2	26	17	} 24	17	21	0.182	0.135*	0.142**	0.142	0.165
7/2	31	31	32	27	27	0.231	0.264*	0.272	0.243	0.228
9/2	5.0	Obscured by other groups	~ 3	2.5	3.5	0.269		0.185	0.164	0.216
11/2	0.7		1.35	1.7	< 1.25	0.045		0.097	0.130	< 0.090

* Normalized such that C^2_{jl} for the spin 1/2 member is the same as that in Yb^{171}.

** Assumes that the unresolved triton groups due to the 3/2 and 5/2 spin members have an intensity ratio of 1:3 similar to that in the other isotopes.

members of the band. It is expected to be a hole state in all the Yb nuclei studied. The triton spectra of Yb^{167} and Yb^{169} each have prominent peaks which fit into bands similar to what is expected for this orbital. In each case the 3/2 and 7/2 spin members have similar intensities, which are much larger than those of other members of the band. In each of the spectra of Yb^{171}, Yb^{173} and Yb^{175} there is a pair of strong triton groups which, due to their intensity, energy spacing and excitation energy, are probably associated with the $3/2-[521]$ orbital. The variation of the absolute (d, t) cross section of the $7/2\ 3/2-[521]$ state as a function of target mass is shown in Figure 19. The decrease in intensity with increasing mass is attributed to a dilution of the state with inert components as the excitation energy becomes higher. As will be seen later, it is expected that this band will be strongly coupled with the $K = 3/2$ gamma vibration band based on the $1/2-[521]$ orbital, and thus some variations in its properties from one nucleus to another might be expected.

I – *The* $5/2-[523]$ *Orbital*

It has been suggested by JOHANSEN[23] that this orbital appears at an excitation energy of 570 kev in Yb^{169}. As it originates from the $h\,9/2$ shell-model state, the only level with a large value of C^2_{jl} is the spin 9/2 member and thus there are no strongly populated states in the band. However, it is expected that three small peaks of roughly equal intensities corresponding to the 5/2, 7/2 and 9/2 rotational states should be observed. In the triton spectrum of Yb^{169}, Figure 2, weak peaks can be seen at positions corresponding to the excitation energies reported by Johansen for the 5/2, 7/2
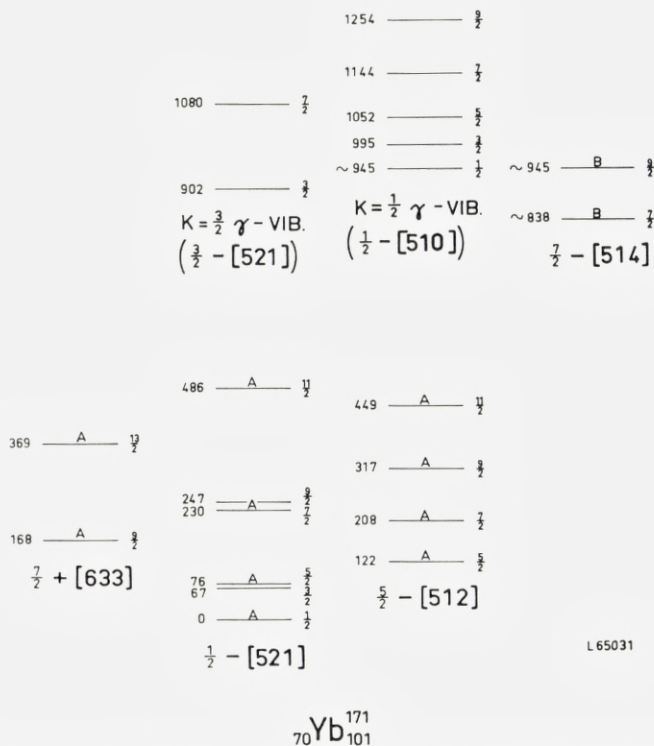
1254 ——— $\frac{9}{2}$

1144 ——— $\frac{7}{2}$

1080 ——— $\frac{7}{2}$ 1052 ——— $\frac{5}{2}$

995 ——— $\frac{3}{2}$

∼945 ——— $\frac{1}{2}$ ∼945 —— B —— $\frac{9}{2}$

902 ——— $\frac{3}{2}$

K = $\frac{3}{2}$ γ-VIB.   K = $\frac{1}{2}$ γ-VIB.   ∼838 —— B —— $\frac{7}{2}$

$\left(\frac{3}{2} - [521]\right)$ $\left(\frac{1}{2} - [510]\right)$ $\frac{7}{2} - [514]$

486 —— A —— $\frac{11}{2}$

449 —— A —— $\frac{11}{2}$

369 —— A —— $\frac{13}{2}$

317 —— A —— $\frac{9}{2}$

247
230 —— A —— $\frac{9}{2}$ $\frac{7}{2}$ 208 —— A —— $\frac{7}{2}$

168 —— A —— $\frac{9}{2}$

122 —— A —— $\frac{5}{2}$

$\frac{7}{2} + [633]$ 76
67 —— A —— $\frac{5}{2}$ $\frac{3}{2}$ $\frac{5}{2} - [512]$

0 —— A —— $\frac{1}{2}$

$\frac{1}{2} - [521]$ L 65031

$_{70}Yb^{171}_{101}$

Figure 14. Level scheme for Yb¹⁷¹. See caption to Figures 12 and 13.

and 9/2 levels. The group due to the spin 7/2 member is not completely resolved from the larger one already assigned to the 3/2 3/2–[521] state. The weak triton group observed at the position where the spin 11/2 state is expected is due largely to another state at about the same energy which is strongly populated in the (d, p) reaction.

The low log ft value for the positron decay of Yb¹⁶⁷ [24, 25] suggests that the 5/2–[523] orbital is the ground state of Yb¹⁶⁷. If one assumes that the highest energy triton group in the spectrum of Figure 1 corresponds to the ground state, the level at 80 kev excitation is probably the 7/2 member of the band, and the group expected for the spin 9/2 state would be obscured by the strong 3/2 3/2–[521] peak.

J – The 5/2 + [642] Orbital

There are three peaks in the triton spectrum of Yb¹⁶⁹ corresponding to excitation energies of 584, 701 and 876 kev which have not yet been discussed. It is noted that, according to the Nilsson scheme, one expects the 5/2 + [642]
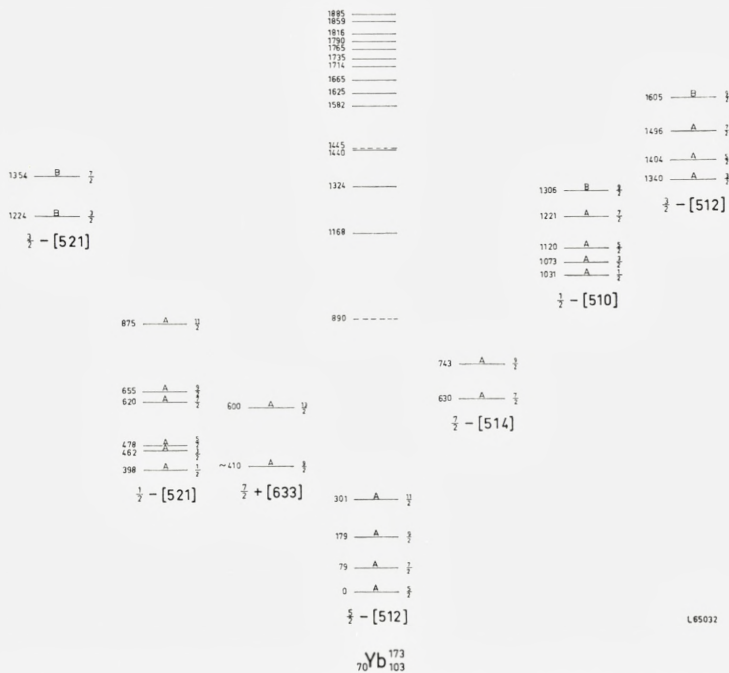
Figure 15. Level scheme for Yb^{173}. See caption to Figures 12 and 13.

state to be found close to the $5/2-[523]$ and $3/2-[521]$ orbitals which occur at 570 kev and 657 kev, respectively, in Yb^{169}. From a comparison of Tables 3 and 9 it is seen that the three triton groups have reasonable intensities to be the 5/2, 9/2 and 13/2 spin members of this band—the 7/2 and 11/2 spin members should be too weakly populated to be seen. This level spacing results in a rather low value of the inertial parameter $\hbar^2/2\mathfrak{J} = 7.3$ kev. However, this is very reasonable for the $5/2+[642]$ orbital which is characterized by a large moment of inertia[2]. On the basis of the present work alone, it is not possible to distinguish between the $5/2+[642]$ and $3/2+[651]$ bands, as Table 9 shows that the predicted intensity patterns are almost identical, and the moments of inertia are probably similar. The choice made above is based on the fact that the $5/2+[642]$ orbital appears higher in the Nilsson scheme and is known to be the ground state of Dy^{161} which has 95 neutrons.

It has been suggested[20] that the $5/2+[642]$ orbital appears at an excitation of 30 kev in Yb^{167}. The spectrum of Figure 1 shows a weak group at this energy, but it seems unlikely that it can be assigned to this orbital due
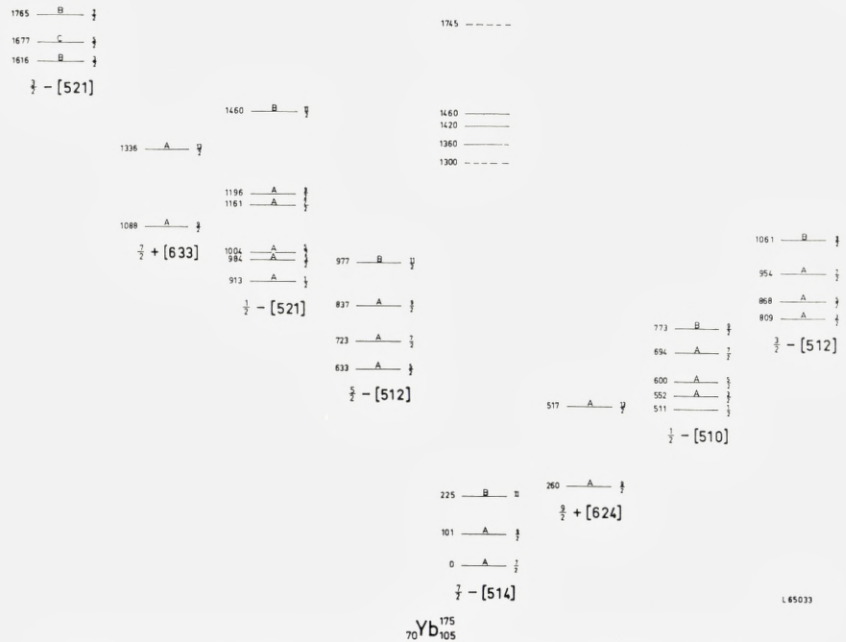
3*

Figure 16. Level scheme for Yb^{175}. See caption to Figures 12 and 13.

to the absence of any triton group corresponding to the spin 9/2 member of the band. If one assumes a moment of inertia similar to that observed in Dy^{161} or Yb^{169}, the 9/2 state should occur at approximately 140 kev. However, there are no triton groups observed between energies corresponding to 79 and 180 kev excitation. Thus, at present there is no good explanation for the levels at 30 kev and 59 kev in Yb^{167}. It is also seen that there are many other unexplained levels in this nucleus. This is perhaps not too surprising as one expects considerable confusion to arise in this region of the Nilsson scheme. First, there should be strong interactions between the pairs of states with the same spin and parity which come from different shells, but which cannot cross each other, namely 1/2 + [660], 1/2 + [400] and 3/2 + [651], 3/2 + [402]. Also there may be considerable Coriolis coupling between pairs of the above bands with K-values differing by unity.

K – Vibrational States

It is a typical feature of the spectra shown in Figures 1–10 that the groups at low excitation energies can be assigned to rotational bands based upon intrinsic states. The relative and absolute populations of these states are
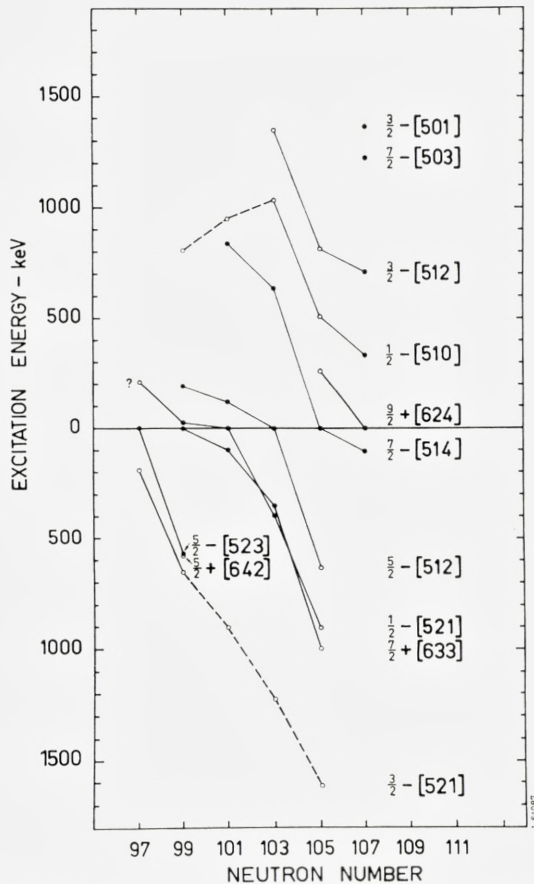
Figure 17. Plot of excitation energies for band heads of the Nilsson states observed. Points shown at negative energies indicate that the orbital is a hole state. Points connected by dashed lines only are those for which the observed cross sections were less than those expected for the pure single-particle transition. These states are interpreted as being collective. See text.

consistent with those expected on the basis of the Nilsson model with pairing effects. However, in each case it is found that the portions of the spectra corresponding to higher excitations cannot be explained in such a simple manner. There are many cases where the Nilsson model would predict the presence of a state which should be strongly populated, but the spectra show no peaks with greater than half the intensity expected for such states. On the other hand, the density of states populated is larger than expected, so that the total differential cross section per Mev of excitation is roughly as
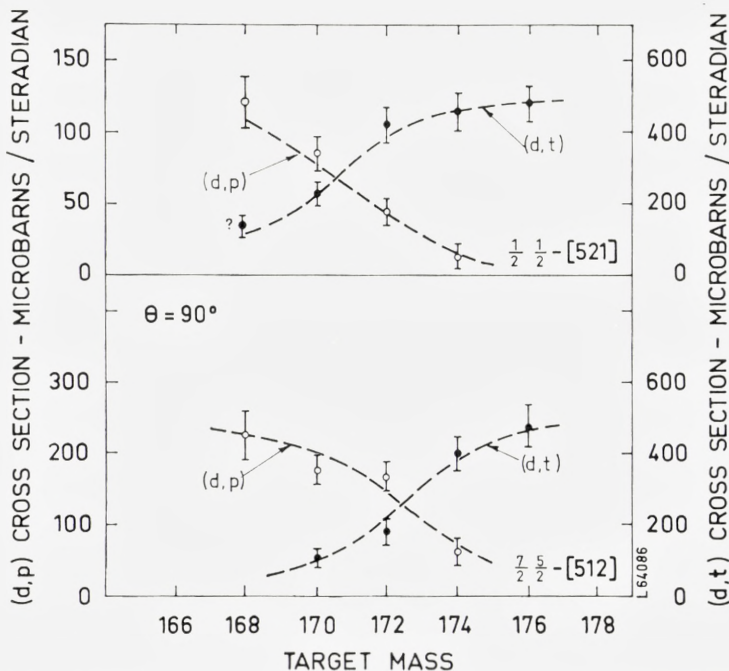
Figure 18. Cross sections for the (d,p) and (d,t) reactions of the $1/2\,1/2-[521]$ and $7/2\,5/2-[512]$ states as a function of target mass number.

calculated for the states which the Nilsson model would predict in this region. It is therefore reasonable to conclude that new modes of excitation become of significance and that the coupling of the single-particle motion to these modes gives rise to a considerable mixing so that the intensity expected for population of a given single-particle state now may be distributed over several states. In this connection it is worth remembering that several collective excitations are found at energies in the neighbourhood of 1 Mev. In the neighbouring even-even nuclei $K = 2+$, gamma vibrational states have been identified in a series of inelastic deuteron scattering experiments[10] which also have given a strong indication for low-lying octupole excitations in this region.

There is a striking correlation between the energies of the low-lying gamma vibrations and the before mentioned break-down of the pure single-particle description. This can be seen in Figure 20 which shows the energy of the most highly excited single-particle state assigned in the previous sections and the energies of the $K = 2+$ gamma-vibrational states in the neighbouring even-even nuclei. Of course it must be expected that the other
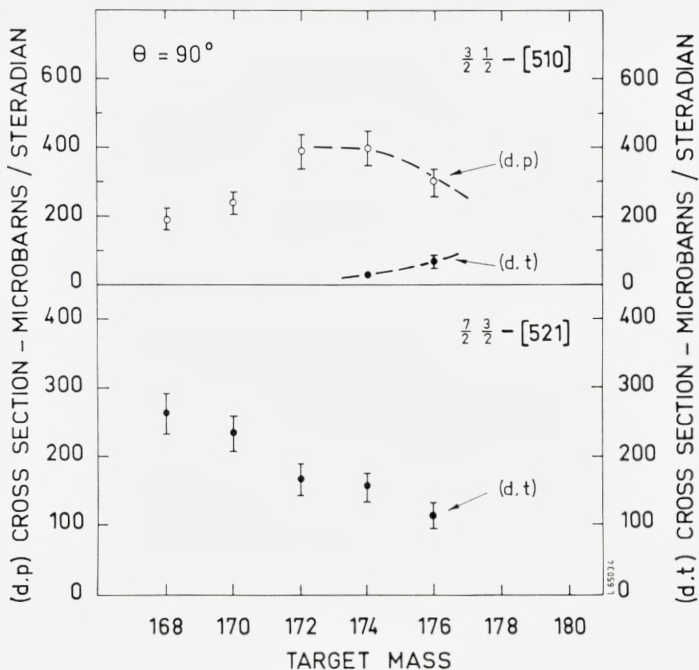
Figure 19. Cross sections for the (d,p) and (d,t) reactions of the $3/2\ 1/2-[510]$ and $7/2\ 3/2-[521]$ states as a function of target mass number.

TABLE 11. Inertial Parameters $\hbar^2/2\mathfrak{J}$ and Decoupling Parameters. Numbers in brackets are decoupling parameters for $K = 1/2$ Bands.

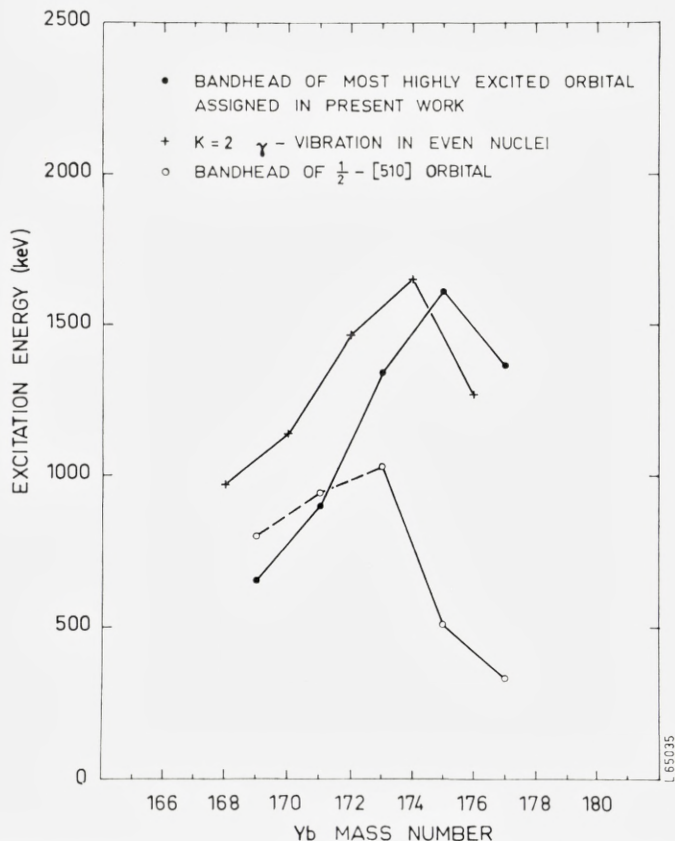| Orbital/Mass	167	169	171	173	175	177
$3/2-[521]$	10.5	12.3	14.7	10.8	12.4	–
$5/2+[642]$	–	7.4	–	–	–	–
$5/2-[523]$	∼ 11.3	11.0	–	–	–	–
$7/2+[633]$	–	8.2	8.4	∼ 7.9	10.3	–
$1/2-[521]$	–	11.5	12.0	12.1	13.5	–
		(0.80)	(0.85)	(0.70)	(0.75)	
$5/2-[512]$	–	12.3	12.2	11.2	12.8	–
$7/2-[514]$	–	–	∼ 11.5	∼ 11.9	11.2	∼ 12.3
$9/2+[624]$	–	–	–	–	10.7	11.0
$1/2-[510]$	–	13.2	12.4	11.9	11.4	12.2
		(0.08)	(0.032)	(+0.20)	(+0.20)	(+0.22)
$3/2-[512]$	–	–	–	12.8	12.0	∼ 12.9

Figure 20. Plot showing the relationship between the region of excitation energy where observed states can be explained with a single-particle description and the gamma vibrational energy.

collective modes have a similar effect, but in the Yb nuclei the spacings of the single-particle states are such that levels connected by large E2-matrix elements occur separated by approximately the phonon energy (cf. Figure 17). Under such conditions a strong coupling of the particle motion to the vibrational motion is highly probable.

A qualitative understanding of some of the coupling phenomena and their significance for the observed stripping and pick-up spectra can be obtained from simple microscopic pictures of the vibrational state. The vibrational state in the even-even nucleus is a superposition of various two-quasiparticle states where the quasiparticles (in the case of the gamma vibration) have K-values differing by two units (Fig. 22). In a collective state many two-

TABLE 12 A. (d, t) Population of $5/2 - [512]$ Band.

Spin	Relative Intensity $\theta = 90°$				Values of C_{jl}^2			
	Theory	Yb^{171}	Yb^{173}	Yb^{175}	Theory	Yb^{171}	Yb^{173}	Yb^{175}
5/2	1.3	3.4	4.4	5.2	0.01	0.022	0.029	0.037
7/2	100	100	100	100	0.786	0.681	0.696	0.742
9/2	2.4	3.5	2.4	1.4	0.141	0.177	0.124	0.077
11/2	1.0	2.2	2.7	2.4	0.062	0.120	0.150	0.142

TABLE 12 B. (d, p) Population of $5/2 - [512]$ Band.

Spin	Relative Intensity $\theta = 90°$				Values of C_{jl}^2			
	Theory	Yb^{169}	Yb^{171}	Yb^{173}	Theory	Yb^{169}	Yb^{171}	Yb^{173}
5/2	1.2	2	~ 4.6	4.8	0.01	0.015	0.03	0.03
7/2	100	100	100	100	0.786	0.72	0.66	0.61
9/2	2.5	3.5	3.8	4.2	0.14	0.18	0.17	0.18
11/2	1.2	1.8	3.4	~ 4.2	0.06	0.09	0.14	0.18

quasiparticle states enter, but the major contributions come from quasi-particles near the Fermi surface. The importance of a given particle combination can be estimated on the basis of the asymptotic quantum numbers $[Nn_z\Lambda]$.

The E2-matrix element vanishes unless $\Delta N = 0$ (or ± 2), $\Delta n_z = 0$, $\Delta \Lambda = 2$ and $\Delta \Sigma = 0$. If these selection rules are fulfilled the matrix element is approximately proportional[27] to $(n + \Lambda + 2)(n - \Lambda)$ where $n = N - n_z$. The amplitude of a given two-quasiparticle state furthermore depends on the single-particle energies and the U and V factors for the corresponding states. Figure 21 shows for Yb^{172} the most important amplitudes in the gamma vibration[26] involving the neutron orbits of interest in this work.

In the odd nuclei one can attempt to describe the vibrational states as superpositions of one-quasiparticle and three-quasiparticle states. The three-quasiparticle states consist of the ground-state particle in the orbit K_g and (one of) the various two-quasiparticle configurations with $(K, K \pm 2)$ which make up the even-even gamma vibration. These states normally cannot be created from an even-nucleus ground state by the addition or subtraction of one nucleon (Fig. 22) and are therefore not populated by the (d, p) or (d, t) reactions. The components of the even vibration which involve a particle in the state $-K_g$, play a special role. In the even vibration the state

TABLE 13. (d,p) Population of $1/2-[510]$ Band.

Spin	Relative Intensities $\theta = 90°$					Relative Values of C_{jl}^2**				
	Theory	Yb^{171}	Yb^{173}	Yb^{175}	Yb^{177}	Theory	Yb^{171}	Yb^{173}	Yb^{175}	Yb^{177}
1/2	2.4	Obscured	3.3	*	3.0	0.01	–	0.01	–	0.01
3/2	100	100	100	100	100	0.40	0.34	0.31	0.31	0.32
5/2	35	43	51	45	48	0.29	0.31	0.33	0.29	0.32
7/2	25	16	25	20	19	0.19	0.10	0.15	0.12	0.12
9/2	1.36	4.4	4.2	5.5	4.5	0.09	0.24	0.21	0.28	0.23
11/2	0.24	Not Observed				0.01	–	–	–	–

* Obscured by $13/2$ $9/2+[624]$.
** The values obtained from experimental results have been normalized such that the sum of C_{jl}^2 for the observed peaks is equal to unity. The error in normalization due to inability to observe the spin $11/2$ states is $< 15\%$ in Yb^{173} and Yb^{175}.

K_g could enter if it is connected with states $K_g \pm 2$ by large E2-matrix elements. In the odd nucleus the same matrix elements will admix the single-particle states $K_g \pm 2$ into the vibrational wave function and these components can be populated by the transfer reactions (Fig. 22). The amplitude of each component depends on the E2-matrix element connecting the states K_g and $K_g \pm 2$ and the important admixtures can therefore be localized in Figure 21. Furthermore, as pointed out, the admixtures are expected to be especially strong when the vibrational energy is close to the single-particle energies of the states $K_g \pm 2$.

Reference to Figure 21 shows that in the Yb nuclei the $5/2-[523]$ and the $3/2-[521]$ states are expected to be components of the gamma-vibrational states on the $1/2-[521]$ state. Similarly, the $1/2-[510]$ state should be a component of the $K-2$ vibration on the $5/2-[512]$ state.

Several of the experimental observations are indicative of effects of the nature discussed above. The most advantageous place to begin comparison may be Yb^{171}. This nucleus has been studied by both the (d,p) and (d,t) reactions and is furthermore a stable nucleus where additional information about the collective states can be obtained from (d,d') experiments. The vibrations based on the $1/2-[521]$ ground state have $K = 3/2$ and $5/2$. It is observed that the lowest band excited in the inelastic scattering experiments coincides in energy, within the experimental error, with the band assigned above as having a large admixture of the $3/2-[521]$ orbital. The intensity in the (d,d') spectrum to this band at $\theta = 125°$ is distributed on the $3/2$, $5/2$, $7/2$ and $9/2$ states in the ratios 5×10^{-4}, 8×10^{-4}, 2×10^{-4}, and 4×10^{-4} expressed relative to the elastic scattering intensity. For the inelastic scattering to
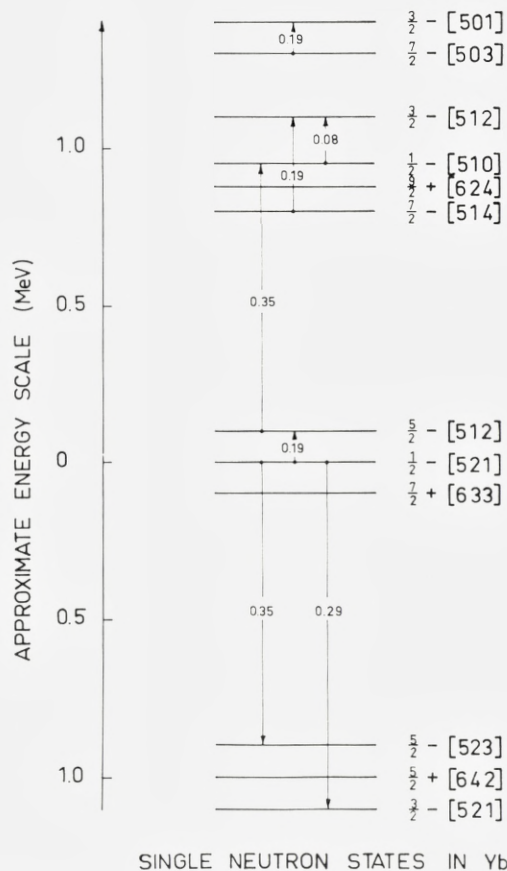
Figure 21. Approximate energy spacings and E2 matrix element strengths between Nilsson states in the Yb region.

the $2+$ and the $4+$, $K = 2$ gamma-vibrational states in Yb^{170} the ratios are 3×10^{-3} and 2×10^{-3}. The total intensity in the odd nucleus is thus approximately 40 % of that in the even nucleus, which is about as expected considering that only half the strength goes to the $K-2$ vibration and one therefore would identify the band as this component. On the other hand, the (d,t) spectrum has a strength to this band which is probably not less than 50 % of that expected for the pure single-particle state (cf. Fig. 19).

The situation is less clear with respect to the $K+2$ component of the gamma vibration. The inelastic deuteron spectrum in the neighbourhood of 1 Mev contains several peaks which could belong to this band. However,
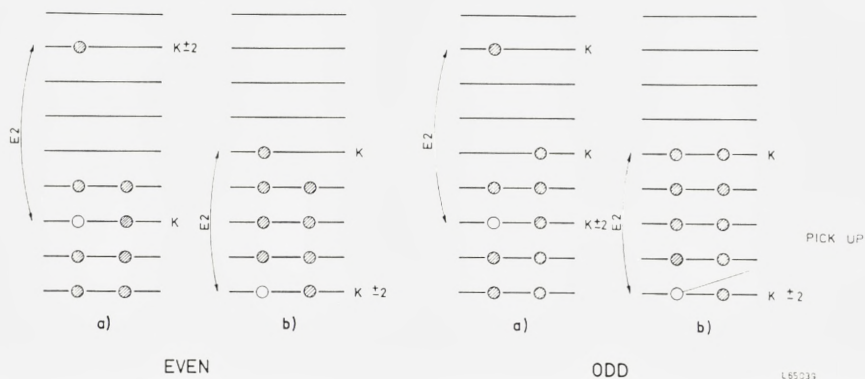
Figure 22. Independent-particle picture of the stripping reaction leading to vibrational states.

the (d,t) intensity to the expected $5/2-[523]$ admixture is weak, and it has not been possible of identify this band.

The other low-lying intrinsic state in Yb^{171} is the $5/2-[512]$ orbital. It is coupled with a strong matrix element to the $1/2-[510]$ orbital, which is a particle state and thus should be seen in the proton spectrum. The previous discussion on the $1/2-[510]$ orbital mentioned a group of levels in Yb^{171} whose intensity pattern resembled that band but whose absolute intensity was only $\sim 60\%$ of the expected value for that orbital. It is interesting to speculate that this might be the $K = 1/2$ gamma-vibrational band based on the $5/2-[512]$ state. It is seen from Table 11 that the decoupling parameter for this band is much smaller than the value of ~ 0.2 observed for the $1/2-[510]$ orbital in the heavier Yb nuclei. This is consistent with the fact that $K = 1/2$ vibrational states usually have small decoupling parameters.

TABLE 14. (d,p) Population of $3/2-[512]$ Band.

Spin	Relative Intensity				Relative Values of C_{jl}^2*			
	Theory	Yb^{173}	Yb^{175}	Yb^{177}	Theory	Yb^{173}	Yb^{175}	Yb^{177}
3/2	26.4	61	45	77	0.08	0.11	0.09	0.15
5/2	100	100	100	100	0.64	0.39	0.42	0.41
7/2	18.9	54	49	51	0.118	0.20	0.20	0.21
9/2	2.9	< 9.5	< 8.5	6.9	0.149	< 0.30	< 0.29	0.23
11/2	0.24	Not observed			0.012	–	–	–

* The values derived from experimental results are normalized such that the sum of C_{jl}^2 for the observed peaks is equal to unity.

Figure 20 also shows the variation of the excitation energy of the $1/2-$[510] orbital with mass number. It is seen that in Yb^{173}, Yb^{175} and Yb^{177}, this state does not appear at an energy close to that which would be expected for the gamma vibration based on the $5/2-$[512] orbital. This is probably the reason why the $1/2-$[510] band appears as a good particle state in these nuclei. However, as one goes down in mass to Yb^{171}, the excitation energy of the $1/2-$[510] orbital approaches that of the gamma vibrations and, as a result, the mixing becomes appreciable.

On the basis of these arguments, one would expect the behaviour in Yb^{169} to be similar to that in Yb^{171}. This is, in fact, seen to be the case, except that the band ascribed to the vibrational state has an intensity only $\sim 45\,^0/_0$ of that which would be expected for the pure $1/2-$[510] state. It is also interesting that another band similar in structure to the $1/2-$[510] orbital, but with an intensity $\sim 40\,^0/_0$ of that expected for the pure state, is seen at higher excitation. The lowest band has a small decoupling parameter (see Table 11) whereas the other has $a = 0.12$, a value comparable to that of the pure state in the heavier Yb nuclei.

One further observation which supports this line of reasoning concerns the results of the Dy^{164} (d,p) Dy^{165} study by SHELINE et al.[22] as re-interpreted in the light of experiments by SCHULT et al.[28]. The latter workers have assigned a $K = 1/2$ band at excitation energy 570.25 kev to be the gamma vibration based on the $5/2-$[512] orbital. The $3/2$ member of this band is at 605.10 kev. In the (d,p) reaction[22], $3/2$ and $5/2$ states at 605 and 658 kev, respectively, are populated. Although intensity values were not given for these proton groups, the relative peak heights in the spectra shown are comparable with those found at a similar reaction angle for the analogous band discussed above in the isotone Yb^{169}. This provides the missing link which connects the bands assumed to be vibrational states in the present work with a band in Dy^{165} assigned as a gamma-vibrational band on the basis of gamma-ray studies.

In conclusion one can say that the experimental observations are in agreement with the qualitative arguments given in the introduction to this section. However, it remains to be seen whether the microscopic theories of nuclear vibrations presently in use can account for the large single-particle amplitudes determined from the observed intensities of the stripping and pick-up reactions.

5. Determination of Δ from the U^2 and V^2

The data shown in Figure 18 have been interpreted above as being an indication of the filling of the $1/2-[521]$ and $5/2-[512]$ orbitals as a function of target mass. If the portions of the curves where the (d, t) cross sections have "saturated" at maximum values are, as assumed, to correspond to V^2 almost unity, the V^2 for these states in the other isotopes can be derived from the figure. Similarly, estimates of the U^2 can be obtained from the (d, p) cross sections. Figure 19 shows, however, that this procedure cannot be applied to states which become badly mixed before the excitation energy is high enough to give the state almost pure hole or particle characteristics.

In order to obtain a value of the parameter Δ from these estimates of the U^2 and V^2, it is useful to consider the standard equations of pairing theory:

$$E_\nu = \sqrt{\Delta^2 + (\varepsilon - \lambda)^2},$$

where E_ν is the quasiparticle energy, ε is the single-particle energy without pairing, and λ is the Fermi energy.

Thus, the excitation energy of a quasiparticle level above the ground state is

$$E = \sqrt{\Delta^2 + (\varepsilon - \lambda)^2} - \sqrt{\Delta^2 + (\varepsilon_0 - \lambda)^2} = \sqrt{\Delta^2 + (\varepsilon - \lambda)^2} - E_0,$$

where ε_0 refers to the ground state. As $\varepsilon_0 - \lambda << \Delta$ the value of E_0 should be approximately equal to Δ.

If one combines the above equation with the usual expression for V^2,

$$V^2 = 1/2\left(1 - \frac{\varepsilon - \lambda}{\sqrt{\Delta^2 + (\varepsilon - \lambda)^2}}\right),$$

TABLE 15. (d, t) Population of $7/2 + [633]$ Band.

Spin	Relative Intensity $\theta = 90°$				Relative Values of C_{jl}^2*			
	Theory	Yb^{169}	Yb^{171}	Yb^{175}	Theory	Yb^{169}	Yb^{171}	Yb^{175}
7/2	1.2	Not seen			0.001	–	–	–
9/2	83	~ 100	79	110	0.07	0.08	0.07	0.09
11/2	1.8	Not seen			0.015	–	–	–
13/2	100	100	100	100	0.915	0.92	0.93	0.91

* The values derived from experimental results are normalized such that the sum of C_{jl}^2 for the observed peaks is equal to unity. The error in normalization due to inability to observe the spin 7/2 and 11/2 states is less than 10% in all cases.
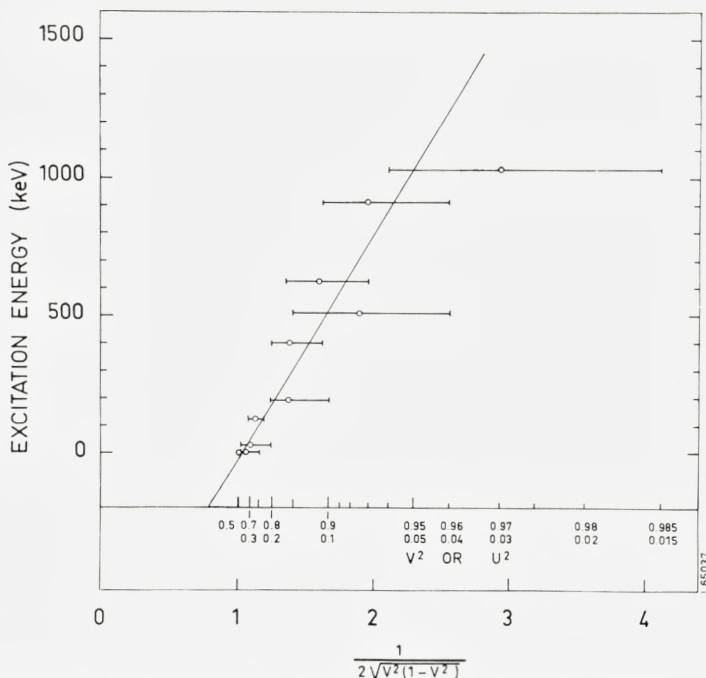
Figure 23. The relationship between the excitation energy of a state and its V^2 (or U^2). Energies are taken from odd nuclei and the values of V^2 (or U^2) were interpolated from values in neighbouring even-even nuclei. Pairing theory suggests that the points should fall on a straight line with slope Δ. The line shown in the figure has a slope of 800 ± 150 kev.

and eliminates $\varepsilon - \lambda$, it is found that

$$E = \frac{\Delta}{2\sqrt{V^2(1 - V^2)}} - E_0.$$

That is, if one plots the excitation energy versus $1/2 \times (V^2(1 - V^2))^{-1/2}$, the points should fall on a straight line with slope Δ and intercept $-E_0$ on the energy axis. Figure 23 shows such a plot for some of the states in the Yb nuclei. The straight line drawn through the points has a slope of 800 kev. The value of Δ thus obtained is 800 ± 150 kev, which is in good agreement with the value of 700 kev derived from the neutron separation energies in this region. It is also noted that the straight line drawn in Figure 23 passes through the point (1,0), which means that the intercept on the energy axis is approximately equal to $-\Delta$, as was to be expected.

6. Comparison of Intensities with Predicted Values

The comparisons of theoretical and experimental relative intensities given in Tables 10–15 show that the main features of the stripping and pick-up processes are described very well by the Nilsson wave functions and the distorted wave calculations. It is noted, however, that there are several cases where the relative cross section of a particular member of a band may be consistently too large or too small when compared to the predicted value. It would be interesting to look for systematic trends in these discrepancies and to try to find their origin. Also, the above discussion has been mainly concerned with relative intensities and a detailed comparison of absolute intensities with predictions has been avoided so far. Of course, in order to make an estimate of an absolute intensity, it is also necessary to have a knowledge of the quantity V^2 and, as we have seen, the purity of the state. From Figure 18, however, it is probably safe to conclude that for the $5/2-$ [512] and $1/2-$[521] orbitals the value of V^2 is nearly unity for the Yb^{176} and Yb^{174} targets, respectively. Similarly, other cases can be found where the V^2 (or U^2) for a band can be assumed to be close to unity for the (d,t) (or (d,p)) reaction. For cases selected in this manner, Figure 24 shows the ratio of experimental to predicted differential cross section at $\theta = 90°$ plotted as a function of l-value for the (d,t) and (d,p) processes. The solid lines in this figure connect points which are obtained by geometrical averaging of all the data points for a particular l-value. It is seen that for the (d,t) case especially, the average values are dependent upon the l-value and are always greater than unity. The fact that the predictions and experiment are in better agreement for the (d,p) process is probably a reflection of the fact that the triton potentials are not as well known as the proton potentials and thus there is more uncertainty in the choice of parameters for the DWBA calculation.

It is also seen that there is a great deal of "scatter" from the average values in Figure 24. Apart from experimental inaccuracies there are various effects which could cause differences between the calculated and the observed cross sections. Several such effects can be imagined: Inelastic effects in the reaction process, a possible dependence on the quantum number j of the stripped particle, band mixing, and the fact that the Nilsson wave functions are approximations. The incoming deuteron could excite the nucleus before the stripping (or pick-up) takes place, and this could give a different distribution of intensity among the final spin states. The triton or proton resulting from the reaction could also cause similar inelastic effects as it leaves the nucleus. It is known from the inelastic deuteron spectra obtained in the present study that, at $\theta = 90°$, inelastic scattering from the first $2+$
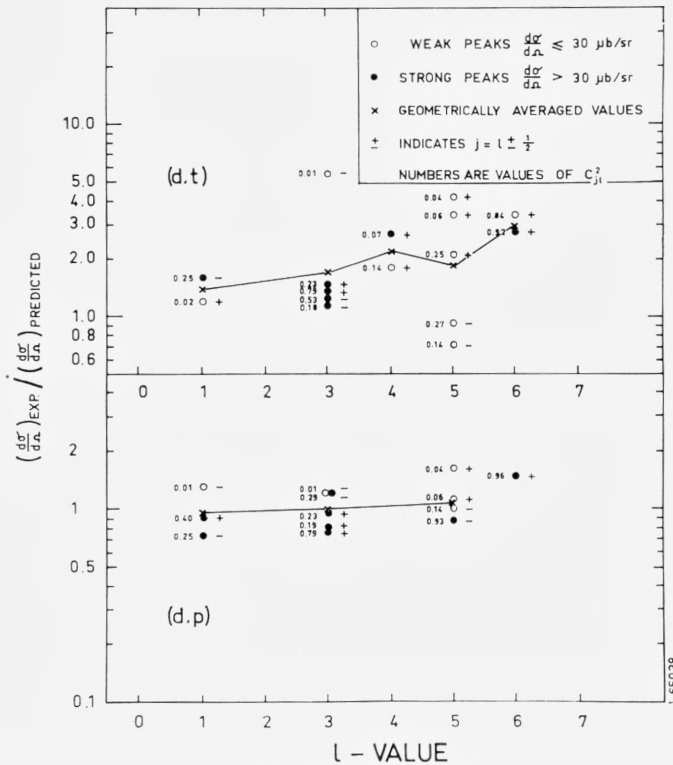
Figure 24. Ratio of experimental to theoretical cross sections for states populated by $(d.p)$ and (d,t) reactions. See text for discussion of discrepancies between experiment and theory.

rotational state in the target nucleus occurs with a probability about 10% of that for elastic scattering. Thus, one should expect that not more than a similar fraction of the intensity of one peak in a band would be redistributed over the other members of the band by such inelastic effects. However, many of the small peaks where discrepancies are observed have intensities from 1% to 5% of that of the strongest peak in the band. The net result of this type of inelastic effect would generally be an increase in intensity of the weakest peaks. Indeed, there does seem to be a slight tendency for the weakly populated states to have higher values in Figure 24 than the strongly populated ones. For the $1/2-[510]$ band, however, it was seen that rotational excitation and stripping lead to an overestimate of the cross section for the $1/2$ state. It is therefore obvious that other effects must also be present.

In Figure 24, one can also look for indications of a j-dependence in the stripping process. If such an effect were present, one might expect a correlation between the directions of the deviations from the average values

and whether the neutron spin is parallel or antiparallel to the orbital angular momentum. The spin direction is indicated by a plus or minus sign beside each point in Figure 24. As points with both signs have random directions of deviation for any l-value, there appears to be no evidence for strong j-dependence in these stripping and pick-up reactions. Strong band mixing between the 1/2–[510] and the 3/2–[512] orbitals has been observed in the tungsten isotopes[5]. In the Yb isotopes, the larger energy differences between these orbitals reduce the mixing so that there appears to be no observable Coriolis mixing. The spacings of orbitals with $\Delta K = \pm 1$ are sufficiently large in the Yb isotopes to obviate detailed consideration of Coriolis coupling in the analysis of the data. Any other mechanism which produces band mixing is also expected to depend upon the separation of the bands. Since the separations vary with nucleus, consistent deviations from the theoretical values for the C_{jl} are probably not due to band mixing.

The Nilsson wave functions are of course approximations and some deviations between the experimental and theoretical values of C_{jl}^2 are expected. If the C_{jl}^2 for a state is large, its relative error should be small. However, if the C_{jl}^2 is small, a considerable relative error can be expected because of greater sensitivity to the choice of parameters in the Nilsson model. Thus, errors of this nature would be expected to result in larger deviations (of either sign) from the averages in Figure 21 for states with small C_{jl}^2 than for those with large C_{jl}^2. In Figure 24, the numbers shown beside the data points show the value of C_{jl}^2 for that state. It is seen that the states with small C_{jl}^2 tend to have large deviations from the average and the direction of the deviation is random. Hence, some of the discrepancies may be due to small errors in the wave functions used. A favourable opportunity for the study of such effects might be offered by the 5/2–[512] band where the 5/2 and 7/2 states have the same V^2 and l-value. The 5/2 state is expected to be populated with an intensity only about 1 % of that of the 7/2 state, but Tables 12 A and 12 B show that the observed population is usually about 4 %. If the discrepancy were due to inelastic effects, one would expect approximately the same amount of distortion of the intensity pattern in each nucleus where the band was observed. Table 12 B indicates, however, that in Yb[169] the intensity ratio in this band is only 2 %, and thus it is more likely that the deviation from the theoretical ratio is a nuclear effect. In this case, it is not unlikely that the theoretical value of C_{jl}^2 could be slightly in error (and could vary from one nucleus to another) as it is rather sensitive to the parameters of the Nilsson model. This is seen when one compares the value of $C_{jl}^2 = 0.01$ calculated from the Nilsson wave functions[1] with that of $C_{jl}^2 = 0.04$ calculated from the wave functions for proton states in the

$N = 5$ shell by MOTTELSON and NILSSON[2]. Although the latter value is applicable only for proton states, it does show that the small values of C^2_{jl} can be rather sensitive to the choice of parameters in the Nilsson model.

This does not mean, however, that in all cases the experimental values are more accurate than the theoretical ones. A simple test in the case of $K = 1/2$ bands is to calculate the decoupling parameter, a, from the relationship

$$a = \sum_I (-1)^{I-\frac{1}{2}} (I + \tfrac{1}{2}) C^2_{Il}.$$

This is really a very severe test for the experimental data because the intensities for the invariably weak peaks corresponding to the high-spin states are weighted much more heavily than those for the low-spin states. For instance, in the $1/2-[521]$ band, the spin $11/2$ state is populated only about 1% as strongly as the spin $1/2$ state, but its contribution in the calculation of the decoupling parameter is several times greater than that of the spin $1/2$ state. When one uses the empirical values of C^2_{jl} from Table 10 in the above expression, it is found that $a = -0.1$, -0.3 and $+0.4$ in Yb^{171}, Yb^{173} and Yb^{175}, respectively. The corresponding values obtained from energy level spacings are $a = +0.87$, $+0.70$ and $+0.67$, respectively, which are in reasonable agreement with the predicted value of 0.9, obtained from the theoretical values of C^2_{jl}. Slightly better agreement can be obtained for the empirical values if correction factors for φ_l for the various l-values obtained from the curves in Figure 24 are used. This procedure should, in fact, give more realistic values for C^2_{jl} than those presented in Tables 10–15. It has not been applied to the data in these tables because the limited experimental data available do not yet give a good determination of the correction factors to be applied to the φ_l. The fact that this procedure still does not predict acceptable values for the decoupling parameter probably indicates that some small effects are present which have not been included in the description of the reaction process.

The above discussion indicates that the small discrepancies observed between experiment and theory cannot be ascribed to any single cause. The most likely causes are uncertainties in the calculated values of φ_l, uncertainties in the nuclear wave functions, and higher order effects in the reaction processes. It is to be remembered, however, that the general agreement between experiment and theory is quite good and is more than adequate to permit unambiguous assignments of bands in cases where mixing is not serious. As can be seen from Figure 24, the discrepancies are only appreciable for those cases where the intensity is less than 5–10 % of that of the strongest peaks in the spectrum.

7. Summary

In the preceding sections it has been seen that the single-nucleon transfer reactions are very useful for the assignment of levels in deformed nuclei because the relative intensities to the various rotational members of a band yield, in effect, the wave function of the intrinsic state. In the present work this technique has resulted in the classification of many previously unknown states in terms of the unified model. The combined use of stripping and pick-up reactions has been very helpful for studying the hole-particle properties of the levels and for determining the U^2 and V^2 factors for various states in the target nuclei. The distributions of neutron pairs among the orbitals near the Fermi surface were found to be in good agreement with pairing theory.

The tentative results concerning the population of vibrational states indicate that these reactions could be used for studying the compositions of such collective states, as each reaction essentially projects out one or two of the various components. This is a problem which deserves further examination and the best suitable nuclei for studies in the rare earth region would probably be the Gd, Dy or Er series. In these nuclei the gamma vibrations occur at lower excitation energies than in the Yb series and their $B(E2)$-values are larger. Under such conditions it is expected that many configurations contribute to the vibration and therefore the amplitude of any single component is much reduced in the total vibrational wave function.

Acknowledgments

The Niels Bohr Institute
University of Copenhagen

References

1) S. G. Nilsson, Mat. Fys. Medd. Dan. Vid. Selsk. **29**, No. 16 (1955).
2) B. R. Mottelson and S. G. Nilsson, Mat. Fys. Skr. Dan. Vid. Selsk. **1**, No. 8 (1959).
3) S. A. Hjorth and B. L. Cohen, Phys. Rev. **135**, B920 (1964).
4) B. L. Cohen and R. E. Price, Phys. Rev. **121**, 1441 (1961).
5) J. R. Erskine, Phys. Rev. **138**, B66 (1965).
6) M. N. Vergnes and R. K. Sheline, Phys. Rev. **132**, 1736 (1963).
7) R. H. Siemssen and J. R. Erskine, to be published.
8) G. R. Satchler, Ann. Phys. **3**, 275 (1958).
9) R. H. Bassel, R. M. Drisko and G. R. Satchler, ORNL Report 3240 (unpublished, and G. R. Satchler, private communication.
10) D. G. Burke et al., to be published.
11) B. Elbek, Determination of Nuclear Transition Probabilities by Coulomb Excitation, (Dissertation), Ejnar Munksgaards Forlag, Copenhagen (1963).
12) Y. Yoshizawa, B. Elbek, B. Herskind and M. C. Olesen, Nucl. Phys. **73**, 273 (1965).
13) J. Borggreen, B. Elbek and L. Perch Nielsen, Nuclear Instr. and Methods **24**, 1 (1963).
14) L. Westgaard and S. Bjørnholm, to be published in Nuclear Inst. and Methods.
15) B. Elbek, M. C. Olesen and O. Skilbreid, Nucl. Phys. **10**, 294 (1959).
16) J. H. E. Mattauch, W. Thiele and A. H. Wapstra, Nucl. Phys. **67**, 32 (1965).
17) G. R. Satchler, private communication.
18) Nuclear Data Sheets, National Academy of Sciences, Washington.
19) B. S. Dzelepov, L. K. Peker and V. O. Sergeyev, Decay Schemes of Radioactive Nuclei, Moscow 1963.
20) O. Nathan and S. G. Nilsson, in Alpha-, Beta- and Gamma-Ray Spectroscopy, Vol. 1. K. Siegbahn, Editor, Amsterdam 1965.
21) C. J. Orth, M. E. Bunker and J. W. Starner, Phys. Rev. **132**, 355 (1963).
22) R. K. Sheline, W. N. Shelton, H. T. Motz and R. E. Carter, Phys. Rev. **136**, B351 (1964).
23) A. Johansen and B. Elbek, to be published.
24) T. Tamura, Nucl. Phys. **62**, 305 (1965).
25) C. Wang et al. JINR-O-1361 (1963).
26) D. R. Bés, P. Federman, E. Maqueda and A. Zuker, Nucl. Phys. **65**, 1 (1965).
27) E. R. Marshalek and J. O. Rasmussen, Nucl. Phys. **43**, 438 (1963).
28) O. W. B. Schult, B. P. Maier and U. Gruber, Z. f. Phys. **182**, 171 (1964).